

Spring 2012

# Study of the Compressive Strength of Aluminum Curved Elements

Christine M. Shepherd  
*Bucknell University*

Follow this and additional works at: [https://digitalcommons.bucknell.edu/honors\\_theses](https://digitalcommons.bucknell.edu/honors_theses)

 Part of the [Civil Engineering Commons](#)

---

## Recommended Citation

Shepherd, Christine M., "Study of the Compressive Strength of Aluminum Curved Elements" (2012). *Honors Theses*. 125.  
[https://digitalcommons.bucknell.edu/honors\\_theses/125](https://digitalcommons.bucknell.edu/honors_theses/125)

This Honors Thesis is brought to you for free and open access by the Student Theses at Bucknell Digital Commons. It has been accepted for inclusion in Honors Theses by an authorized administrator of Bucknell Digital Commons. For more information, please contact [dcadmin@bucknell.edu](mailto:dcadmin@bucknell.edu).



**STUDY OF THE COMPRESSIVE STRENGTH OF ALUMINUM CURVED  
ELEMENTS**

by

**Christine M. Shepherd**

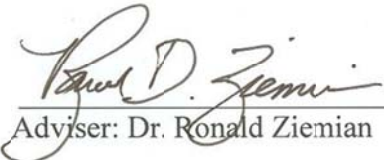
A Thesis Submitted to the Honors Council

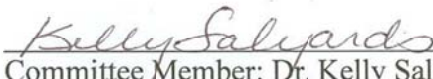
For Honors in Civil Engineering

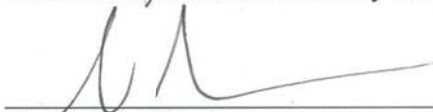
at Bucknell University

May 10<sup>th</sup>, 2012

Approved by:

  
Adviser: Dr. Ronald Ziemian

  
Committee Member: Dr. Kelly Salyards

  
Committee Member: Dr. Sharon Garthwaite

## **ACKNOWLEDGEMENTS**

I would like to thank Dr. Ronald Ziemian for his support through this process. He has served as a professor, adviser and mentor for me as I progressed through my studies. His enthusiasm for structural engineering and his dedication to his students is truly inspiring.

I want to extend a thank you to the other professors who made this endeavor possible with their willingness to help. I would also like to thank my family and friends for helping me through this process as well. I could not have done this without you!

## TABLE OF CONTENTS

LIST OF TABLES .....	v
LIST OF FIGURES .....	vi
ABSTRACT.....	ix
1. INTRODUCTION.....	1
1.1 Objective .....	1
1.2 Scope .....	2
2. BACKGROUND.....	4
2.1 Theory .....	4
2.2 History .....	6
2.2.1 Literature Survey .....	6
2.2.2 Prior Work .....	7
3. DISCUSSION.....	9
3.1 Software .....	9
3.2 Inputs and Assumptions .....	9
4. MODELS AND RESULTS.....	17
4.1 Edge-support Conditions.....	17
4.1.1 Pin-Pin.....	17
4.1.2 Pin-Fixed.....	22
4.1.3 Fixed-Fixed.....	27
4.1.4 Fixed-Free.....	31
4.1.5 Pin-Free.....	35
4.2 Summary of Results .....	39
5. EXAMPLES .....	41
5.1 Example 1.....	42
5.2 Example 2.....	45
6. CONCLUSION .....	47
6.1 Summary .....	47
6.2 Conclusions .....	48
6.3 Future Work .....	49
BIBLIOGRAPHY.....	50
APPENDIX.....	51

## LIST OF TABLES

<b>Table 1.</b> Buckling coefficient formulas for curved panels (LeTran & Davaine, 2011) .....	8
<b>Table 2.</b> Geometries used to test different b/t ratios in CU-FSM .....	13
<b>Table 3.</b> CU-FSM results with output from the nonlinear regression for the pin-pin edge-support condition case .....	20
<b>Table 4.</b> CU-FSM results with output from the nonlinear regression for the pin-fixed edge-support condition case .....	25
<b>Table 5.</b> CU-FSM results with output from the nonlinear regression for the fixed-fixed edge-support condition case .....	29
<b>Table 6.</b> CU-FSM results with output from the nonlinear regression for the fixed-free edge-support condition case .....	33
<b>Table 7.</b> CU-FSM results with output from the nonlinear regression for the pin-free edge-support condition case .....	37
<b>Table 8.</b> Summary of results of nonlinear regression analysis.....	39

## LIST OF FIGURES

<b>Figure 1.</b> Local buckling of a column flange (Kissell, 1995) .....	1
<b>Figure 2.</b> Extruded aluminum shapes used as connectors ( <i>Extrusion</i> , 2007). .....	2
<b>Figure 3.</b> Plate buckling coefficients, $k_c^{plate}$ , for each of the five edge-support conditions considered (Ziemian, 2010).....	3
<b>Figure 4.</b> Geometric properties of curved plate sections used to calculate the curvature parameter, $Z$ .....	4
<b>Figure 5.</b> Sample of aluminum curved shapes as they appear within structural shapes (Kissell, 1995) .....	5
<b>Figure 6.</b> Plate element subject to uniform compression (Kissell, 1995) .....	6
<b>Figure 7.</b> Input screen in CU-FSM with a sample section with $Z=20$ with (a) Material Properties, (b) Node information, (c) Element information and nodes 1 and 33 labeled.....	10
<b>Figure 8.</b> Screenshot of the CU-FSM results including buckled shape, half-wavelength and load factors.....	12
<b>Figure 9.</b> Critical stress ratios for fixed-free edge-support condition analyzed with three b/t ratios .....	13
<b>Figure 10.</b> Range of curvature parameters tested.....	14
<b>Figure 11.</b> Previously considered equations (Table 1) for buckling coefficients verses CU-FSM results for the pin-pin edge-support condition.....	15
<b>Figure 12.</b> Previously considered equations (Table 1) for buckling coefficients verses CU-FSM results for the fixed-fixed edge-support condition.....	15
<b>Figure 13.</b> Buckled shapes for the pin-pin condition at a range of curvature parameters.....	19
<b>Figure 14.</b> Plot of CU-FSM data points and the nonlinear regression model from MATLAB for the pin-pin edge-support conditions with the inset showing the intercept at the flat plate buckling coefficient. ....	21
<b>Figure 15.</b> Critical buckling stress ratio for the pin-pin condition with inset showing the intercept at 1 .....	22

<b>Figure 16.</b> Buckled shapes for the pin - fixed condition at a range of curvature parameters.....	24
<b>Figure 17.</b> Plot of CU-FSM data points and the nonlinear regression model from MATLAB for the fixed-pin edge-support conditions with the inset showing the intercept at the flat plate buckling coefficient .....	26
<b>Figure 18.</b> Critical buckling stress ratio for the fixed-pin condition with inset showing the intercept at 1 .....	26
<b>Figure 19.</b> Buckled shapes for the fixed-fixed condition at a range of curvature parameters.....	28
<b>Figure 20.</b> Plot of CU-FSM data points and the nonlinear regression model from MATLAB for the fixed-fixed edge-support conditions with the inset showing the intercept at the flat plate buckling coefficient .....	30
<b>Figure 21.</b> Critical buckling stress ratio for the fixed-fixed condition with inset showing the intercept at 1 .....	30
<b>Figure 22.</b> Buckled shapes for the fixed - free condition at a range of curvature parameters.....	32
<b>Figure 23.</b> Plot of CU-FSM data points and the nonlinear regression model from MATLAB for the fixed-free edge-support conditions with the inset showing the intercept at the flat plate buckling coefficient .....	34
<b>Figure 24.</b> Critical buckling stress ratio for the fixed-free condition with inset showing the intercept at 1 .....	34
<b>Figure 25.</b> Buckled shapes for the pin - free condition at a range of curvature parameters.....	36
<b>Figure 26.</b> Plot of CU-FSM data points and the nonlinear regression model from MATLAB for the pin-free edge-support conditions with the inset showing the intercept at the flat plate buckling coefficient .....	38
<b>Figure 27.</b> Critical buckling stress ratio for the fixed-fixed condition with inset showing the intercept at 1 .....	38



<b>Figure 28.</b> Buckling coefficients from nonlinear regression analysis versus curvature parameter, $Z$ for each edge-support condition considered in this study .....	40
<b>Figure 29.</b> Critical buckling stress ratios versus curvature parameter for all five edge-support conditions .....	41
<b>Figure 30.</b> Geometry of the section used in Example 1 .....	42
<b>Figure 31.</b> Geometry of the section used in Example 2 .....	45

## ABSTRACT

Currently, the Specification for Aluminum Structures (Aluminum Association, 2010) shows thin-walled aluminum plate sections with radii greater than eight inches have a lower compressive strength capacity than a flat plate with the same width and thickness. This inconsistency with intuition, which suggests any degree of folding a plate should increase its elastic buckling strength, inspired this study. A wide range of curvatures are studied—from a nearly flat plate to semi-circular. To quantify the curvature, a single non-dimensional parameter is used to represent all combinations of width, thickness and radius. Using the finite strip method (CU-FSM), elastic local buckling stresses are investigated. Using the ratio of stress values of curved plates compared to flat plates of the same size, equivalent plate-buckling coefficients are calculated. Using this data, nonlinear regression analyses are performed to develop closed form equations for five different edge support conditions. These equations can be used to calculate the elastic critical buckling stress for any curved aluminum section when the geometric properties (width, thickness, and radius) and the material properties (elastic modulus and Poisson's ratio) are known. This procedure is illustrated in examples, each showing the applicability of the derived equations to geometries other than those investigated in this study and also providing comparisons with theoretically exact numerical analysis results.

# 1. INTRODUCTION

## 1.1 Objective

In structural engineering, local buckling is an important failure mode to be considered in the design of a structural member subject to compression. Local buckling is identified by a portion of a structural shape (typically a web or flange) deflecting over a short region. The effects of local buckling are more severe with larger width-to-thickness ratios ( $b/t$ ). Figure 1 illustrates local buckling and the scale of its effects along a structural member. In this case, the flange of an I-shape buckled after being subject to a compressive force.

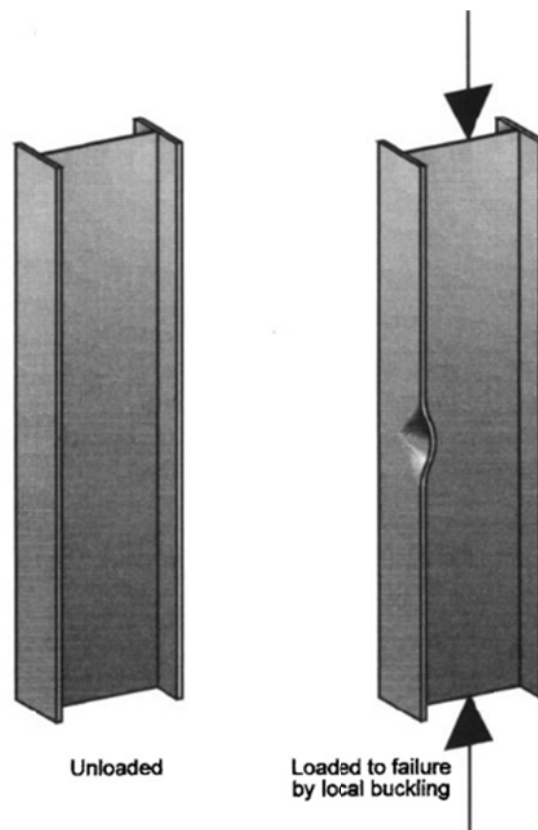


**Figure 1.** Local buckling of a column flange (Kissell, 1995)

Curved elements in extruded aluminum shapes are significantly more common than curved elements in steel due to the ease of fabrication. Curved aluminum sections can be seen in applications such as mullions and façade suspension systems (Figure 2). Therefore, it is important to understand the local buckling behavior of curved elements subjected to uniform compressive loads.

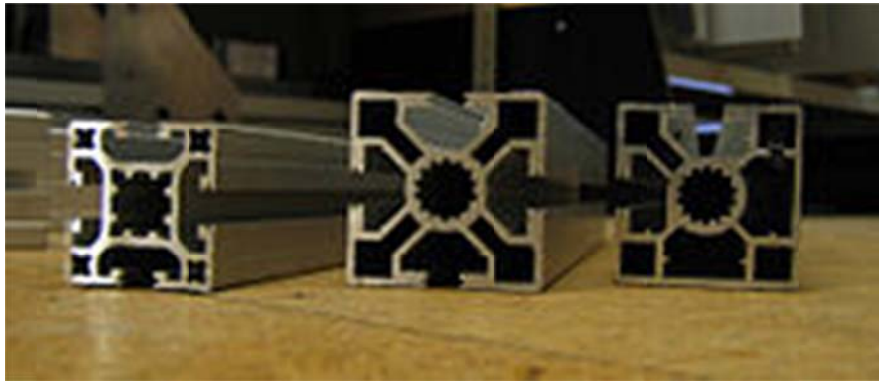


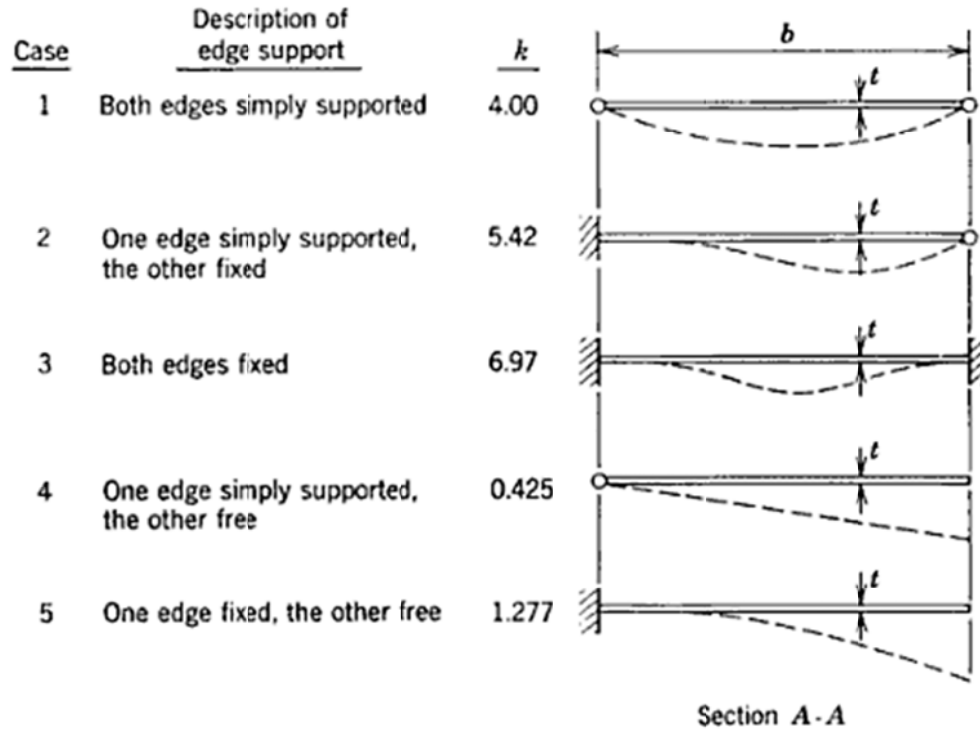
**Figure 2.** Extruded aluminum shapes used as connectors (*Extrusion, 2007*).

The current aluminum specification predicts that sections with a radius greater than eight inches will have a lower strength capacity than a flat plate, which is inconsistent with intuition (Aluminum Association, 2010). In addition to investigating this inconsistency, this study serves to find a simple equation for the elastic critical buckling stress of an aluminum thin plate with a defined width, thickness and radius when subject to uniform compression over a range of edge-support conditions.

## 1.2 Scope

This study aims to develop an expression for a equivalent plate buckling coefficient  $k_c^Z$  that can be used in the determination of the elastic plate buckling stress  $\sigma_{cr}^Z$  in curved cross-sections. To do this, multiple degrees of curvature will be evaluated at

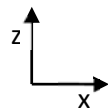
five different edge-support conditions (Figure 3). These edge-support conditions are pin-pin (also labeled as simply-supported), fixed-fixed, fixed-free, pin-free and pin-fixed.



**Figure 3.** Plate buckling coefficients  $k_c^{plate}$  for each of the five edge-support conditions considered (Ziemian, 2010)

To normalize the results for different width-to-thickness ratios and radii, the degrees of curvature will be defined by the non-dimensional parameter  $Z$  (defined in Eq. 1), which is used in LeTran and Davaine's study of the compressive strength of steel curved plates (2011). This  $Z$  factor takes into account the width, thickness and radius of an element as illustrated in Figure 4.

$$Z = \frac{b^2}{Rt} \quad (\text{Eq. 1})$$



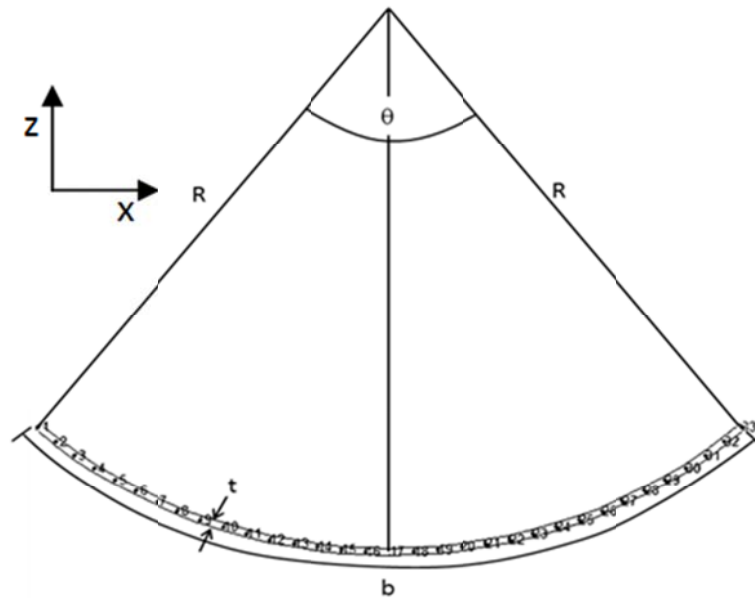


**Figure 4.** Geometric properties of curved plate sections used to calculate the curvature parameter  $Z$

## 2. BACKGROUND

### 2.1 Theory

Local buckling of an element can occur at a lower stress than that at which a compression member experiences flexural and/or torsional buckling. Due to the low moment of inertia and low initial resistance to out-of-plane deformations, thin-walled plate sections, like those often found in extruded aluminum shapes, are particularly susceptible to local buckling (White, Gergely, and Sexsmith 1974). Figure 5 shows examples of curved elements within structural shapes.



**Figure 5.** Sample of aluminum curved shapes as they appear within structural shapes (Kissell, 1995)

The elastic critical stress  $\sigma_{cr}$  of a flat plate is dependent on the width-to-thickness ratio,  $b/t$ , and longitudinal edge-support conditions according to

$$\sigma_{cr} = k \frac{\pi^2 E}{12(1-\nu^2) \left(\frac{b}{t}\right)^2} \quad (\text{Eq. 2})$$

where  $k$  is the plate buckling coefficient (Figure 3),  $E$  is the elastic modulus of the material, and  $\nu$  is Poisson's ratio.

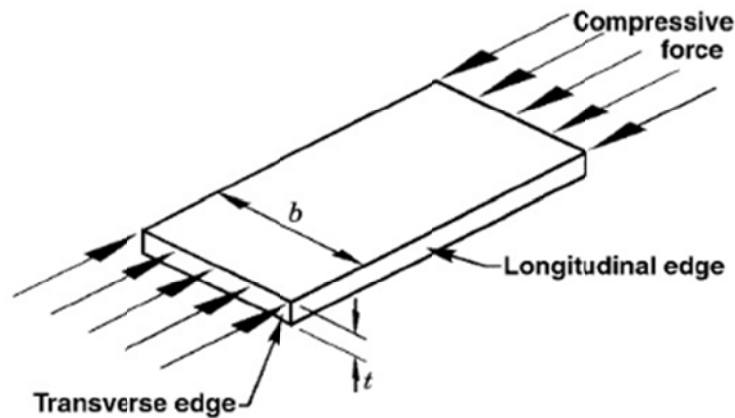


**Figure 6.** Plate element subject to uniform compression (Kissell, 1995)

## 2.2 History

### 2.2.1 Literature Survey

LeTran and Davaine explore local buckling of curved steel plates in their paper, “Stability of curved panels under uniform axial compression” (2011). This study focuses on large scale applications, like steel bridges. The literature survey presented in LeTran and Davaine’s paper is comprehensive and current. Only published one year prior, LeTran and Davaine’s present information gathered historically and currently on curved plate behavior in steel bridges. It also indicates that there are not many studies on the buckling theory of curved panels, especially compared to those on flat plate buckling or cylindrical shell buckling.

Research into the behavior of curved aluminum plates has not been extensively explored. Although the Specification for Aluminum Structures indicates an



inconsistency between flat and curved plates, no work was found to indicate further investigation into aluminum curved plate behavior. This study aims to apply the knowledge from LeTran and Davaine’s paper on curved plate behavior in steel to similar behavior in aluminum.

### 2.2.2 Prior Work

In “Stability of curved panels under uniform axial compression,” LeTran and Davaine (2011) investigated curved steel plates using extensive finite element studies that employ shell elements. The local buckling behavior did indeed depend on curvature, width-to-thickness ratio, and initial imperfections. However, only simple supports applied on four edges were considered.

Four primary equations (seen in Table 1) are studied by LeTran and Davaine and document the evolution of the understanding of curved plate behavior to include edge-support conditions and developments in finite element modeling software (2011). These four equations calculate a buckling coefficient  $k_c^Z$  that includes curvature effects. The critical elastic buckling stress with curvature considered  $\sigma_{cr}^Z$  would then take the form

$$\sigma_{cr}^Z = k_c^Z \sigma_E \quad (\text{Eq. 3})$$

where  $\sigma_E$  is the elastic critical stress as defined above in Eq. 2 with  $k = 1$ . Buckling coefficients for the simply supported edge-support condition as proposed by Redshaw, Timoshenko, Stowell, and Domb and Leigh are investigated. Redshaw and Stowell use similar forms to their equations, whereas Timoshenko makes an assumption on the form of the displacements and Domb & Leigh’s equation is calibrated using a

curve fitting method (LeTran & Davaine, 2011). Stowell's is the only equation to account for different edge-support conditions.

**Table 1.** Buckling coefficient formulas for curved panels (LeTran & Davaine, 2011)

Author (Year)	Expression for buckling coefficient, $k_c^Z$
Redshaw (1933)	$2 \left( 1 + \sqrt{1 + \frac{12(1 - \nu^2)}{\pi^4} Z^2} \right)$
Timoshenko (1961)	$4 + \frac{3(1 - \nu^2)}{\pi^4} Z^2 \quad \text{if } Z \leq \frac{2\pi^4}{\sqrt{3(1 - \nu^2)}}$ $\frac{4\sqrt{3}}{\pi^2} Z^2 \quad \text{if } \frac{2\pi^4}{\sqrt{3(1 - \nu^2)}} \leq Z$
Stowell (1943)	$\frac{k_c^{plate}}{2} \left( 1 + \sqrt{1 + \frac{48(1 - \nu^2)}{\pi^4 (k_c^{plate})^2} Z^2} \right)$
Domb and Leigh (2001)	$10 \sum_{i=0}^3 c_i (\log Z_b)^i \quad 1 \leq Z < 23.15$ $c(Z)^d \quad 23.15 \leq Z \leq 200$ <p>Where <math>Z_b = Z(1 - \nu^2)</math>, <math>c_0 = 0.6021</math>, <math>c_1 = 0.005377</math>, <math>c_2 = 0.192495</math>, <math>c_3 = 0.00267</math>, <math>c = .4323</math>, and <math>d = .9748</math></p>

### 3. DISCUSSION

#### 3.1 Software

The elastic buckling behavior of thin-walled members can be modeled and analyzed through the use of CU-FSM (Schafer, 2006). CU-FSM employs the finite strip method—a specialized form of the finite element method—to find the buckling curve (buckling stress versus wave-length) of a particular cross section. Degrees of freedom are defined at each node, enabling the user to model different edge-support conditions by changing the restraint condition at the edge end nodes. The minima of the buckling curves provide the half-wavelength and load factor for a given buckling mode. Since local buckling is the focus of this study, the buckling mode at the shortest half-wavelength is identified and used in subsequent analyses. The stress distribution is an input parameter in CU-FSM and, when multiplied by the resulting load factor at the minimum of interest, the buckling stress can be determined. The methodology within CU-FSM mirrors that of standard matrix methods of structural analysis. Through the deflected shape images and the buckling curves produced, CU-FSM aids in the understanding of cross-sectional stability of structural members (Schafer, 2006).

#### 3.2 Inputs and Assumptions

To create the input geometries for CU-FSM, a constant width-to-thickness ratio,  $b/t$ , is maintained while the radius,  $R$ , is varied. Each of the thirty-two elements used to

model the cross-section geometry is subject to a uniform compressive stress of 1 ksi, resulting in an applied load ratio equivalent to the elastic critical buckling stress (in ksi). In this analysis, initial imperfections are ignored. Inputs variables include material properties, such as elastic modulus ( $E=10,100$  ksi), Poisson's ratio ( $\nu=0.33$ ) and shear modulus ( $G=3,797$  ksi), as well as the coordinates of each node and properties of the elements, including thickness and node connectivity (Figure 7). Degrees of freedom are specified at each node, with the conditions at the end nodes (in this case, 1 and 33) representing the edge-support conditions of the plate. A longitudinal restraint is denoted as a zero in the  $xdof$ ,  $ydof$ , or  $zdof$  columns where x-, y-, and z- axes are labeled above in Figure 4. A rotational restraint is denoted as a zero in the  $qdof$  column.

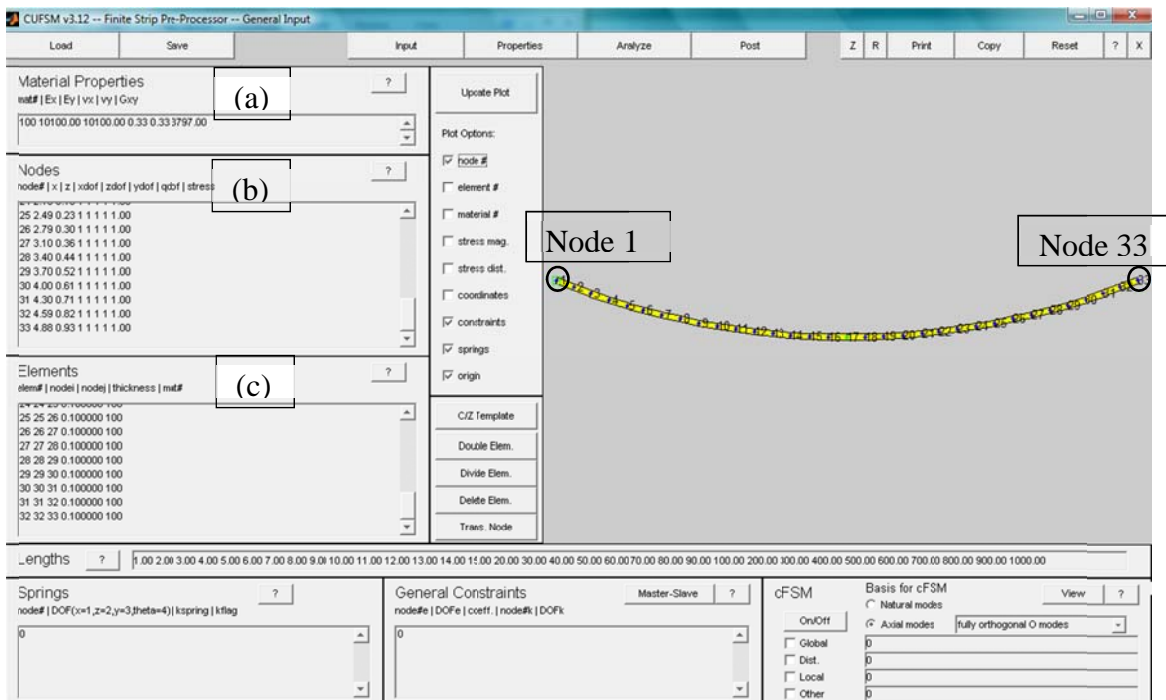


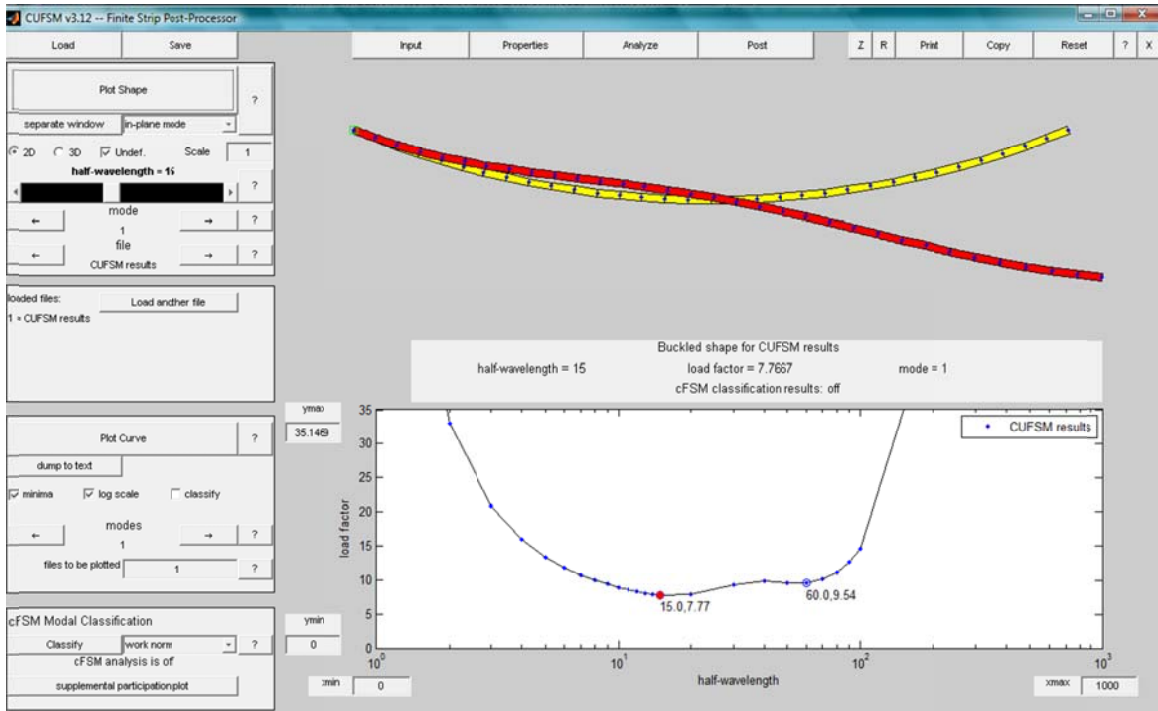
**Figure 7.** Input screen in CU-FSM with a sample section with  $Z=20$  with (a) Material Properties, (b) Node information, (c) Element information and nodes 1 and 33 labeled.

### 3.3 Methodology

CU-FSM is used to analyze curved plate sections for a series of twenty curvature parameter ( $Z$ ) values for each of five edge-support conditions (pin-pin, fixed-free, fixed-fixed, pin-fixed and pin-free). To find the critical elastic buckling stress of interest, the entire buckling stress curve is reviewed in order to target the correct minimum, as more than one may exist (as in Figure 8). The input wavelength range (“Lengths” seen in Figure 7) can be tailored to include the minimum of interest with a narrower range and smaller increment to obtain more accurate wavelengths and load factors. The critical buckling stress is calculated by multiplying the applied stress by the load factor. In this study, the load factor is equal to the critical buckling stress given that the applied stress is 1 ksi. Nearly flat plate behavior is modeled by sections with a curvature parameter of  $Z=0.01$ . Calculating the critical stress ratio  $\sigma_{cr}^Z/\sigma_{cr}^{plate}$  (Eq. 4) eliminates the need to compute the elastic buckling stress when determining the equivalent curved plate buckling coefficient from CU-FSM results.

$$k_c^Z = k_c^{plate} \frac{\sigma_{cr}^Z}{\sigma_{cr}^{plate}} \quad (\text{Eq. 4})$$

Eliminating the elastic buckling stress removes the dependency of the width-to-thickness ratio when generating general equations, thereby allowing for the use of the  $Z$  parameter instead.

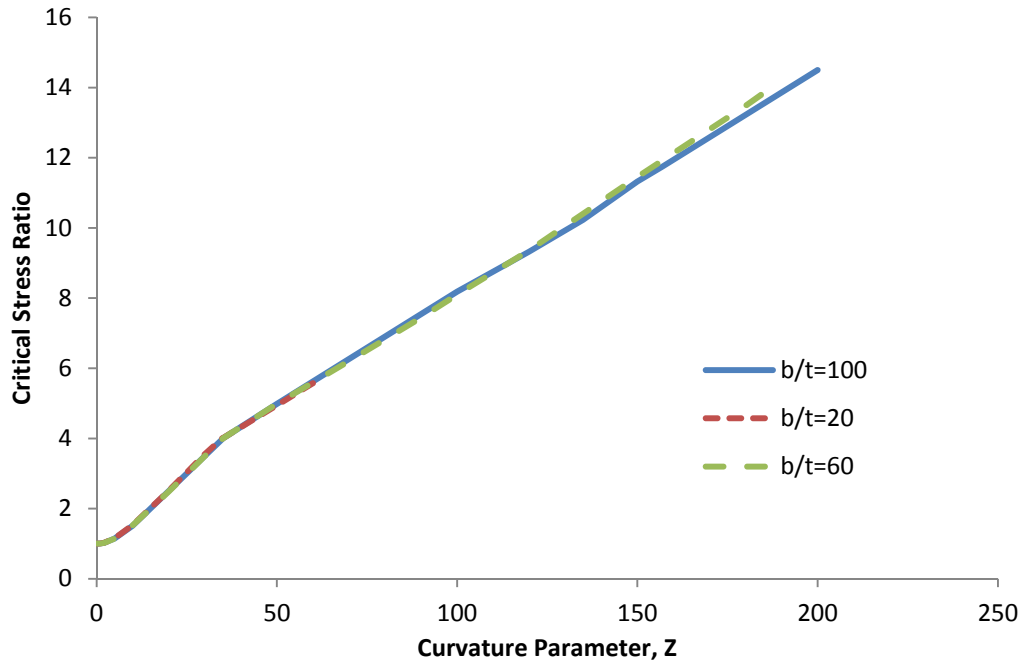


**Figure 8.** Screenshot of the CU-FSM results including buckled shape, half-wavelength and load factors

Before proceeding with the evaluation of different edge-support conditions, the fixed-free support condition was used to ensure the ratio of curved plate critical stress to flat plate critical stress ( $\sigma_{cr}^Z/\sigma_{cr}^{plate}$ ) remained constant over a range of  $b/t$  and corresponding  $Z$ -values. Analyses at each of the  $b/t$  ratios listed in Table 2 were investigated, the results of which are seen in Figure 9. This plot shows the ratio of critical stresses as determined from CU-FSM, remaining constant with different  $b/t$  ratios. Therefore, only one  $b/t$  ratio and a range of radii need be analyzed at each of the subsequent edge-support conditions.

**Table 2.** Geometries used to test different b/t ratios in CU-FSM

Width-to-thickness ratio, b/t	Width, b (inches)	Thickness, t (inches)
100	10	0.1
60	6	0.1
20	10	0.5

**Figure 9.** Critical stress ratios for fixed-free edge-support condition analyzed with three b/t ratios

To test the sensitivity of CU-FSM results to the orientation of the plate, multiple cases were then run with the plate in a horizontal plane ( $b$  along the x-axis in the flat plate condition) and compared to the results when the plate was oriented vertically ( $b$  along the z-axis in the flat plate condition). There was no difference between the results from the two cases with fixed-free edge-support conditions, so only one orientation (parallel to the horizontal plane) is analyzed in this study.

The range of curvature parameters tested was from a flat plate condition ( $Z=0.01$ ) to a semi-circular section ( $Z=314$ ) as indicated in Figure 10.

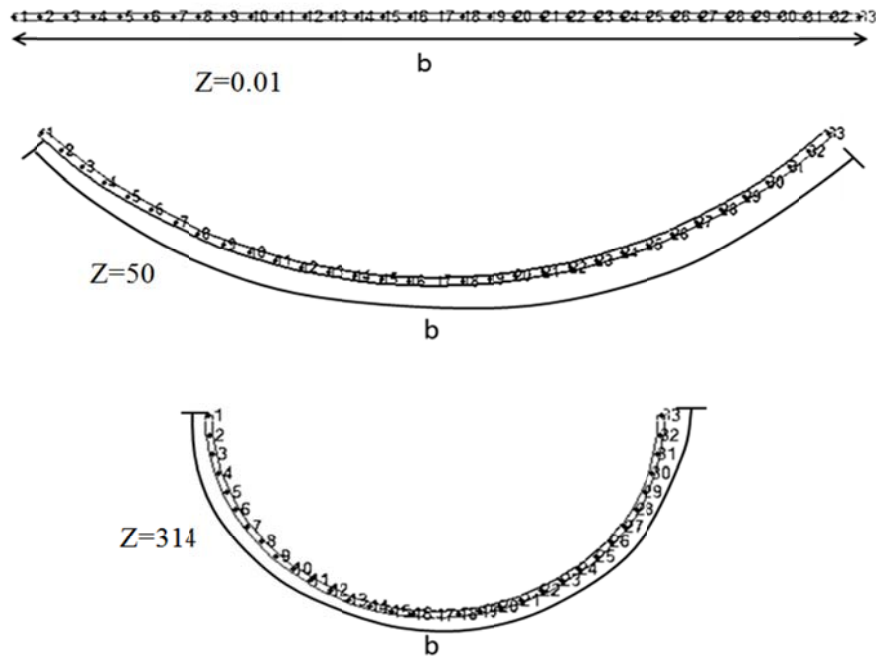


**Figure 10.** Range of curvature parameters tested

CU-FSM data points at each edge-support condition case are plotted against the four equations listed in Table 1. The numerical results aligned best with Redshaw's equation for the buckling coefficient in the pin-pin edge-support condition case (Figure 11), but this equation does not account for different edge-support conditions. As shown in Figure 12 for the fixed-fixed edge-support condition, the analysis results from CU-FSM align best with Stowell's curve for low  $Z$ -values, but at higher curvature parameters, however, the analysis results trend towards Redshaw's curve.



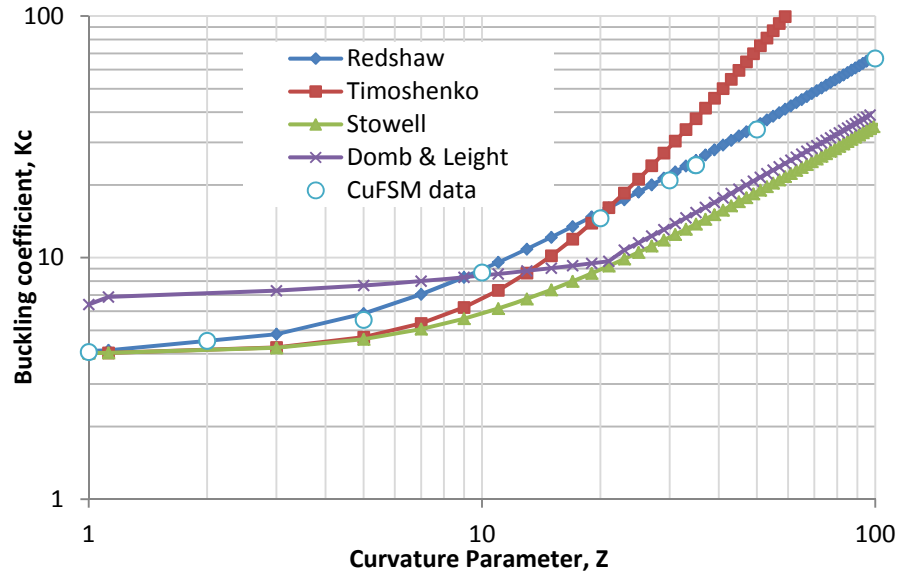


**Figure 11.** Previously considered equations (Table 1) for buckling coefficients verses CU-FSM results for the pin-pin edge-support condition

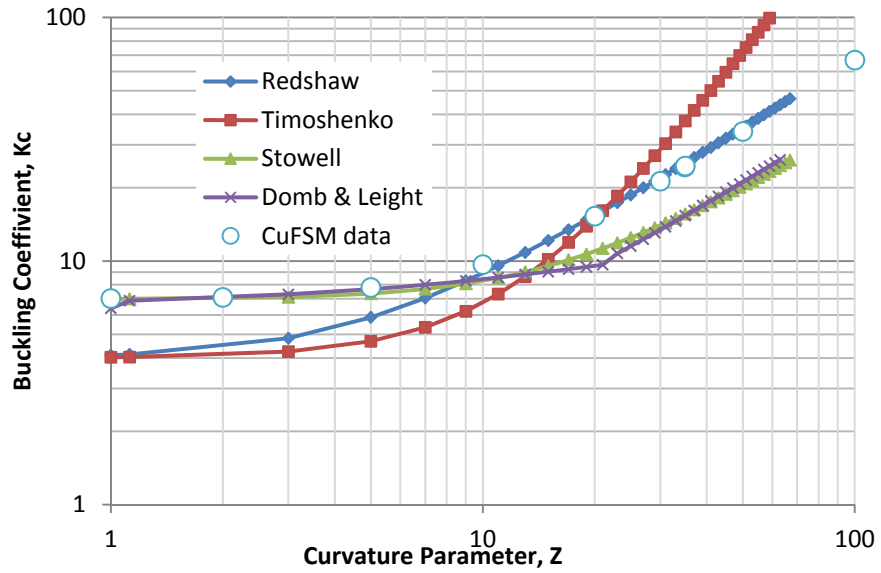


**Figure 12.** Previously considered equations (Table 1) for buckling coefficients verses CU-FSM results for the fixed-fixed edge-support condition

Based on the form of Stowell's and Redshaw's equations and the corresponding shape of the CU-FSM results, an equation of the form

$$k_c^Z = A(1 + \sqrt{1 + BZ^2}) \quad (\text{Eq. 5})$$

is fit to the numerical data using a nonlinear regression analysis, in which  $A$  and  $B$  are the unknown coefficients.

At low curvature parameters ( $Z$  approximately equal to 0.0), the plate in consideration will behave like a flat plate and therefore, the coefficient  $A$  becomes

$$A = \frac{k_c^{plate}}{2} \quad (\text{Eq. 6})$$

where  $k_c^{plate}$  is the flat plate buckling coefficient for the given edge-support condition (see Figure 3). Using the collection of  $Z$  and corresponding  $k_c^Z$  data, the parameter  $B$  is determined through the *nlinfit* function in MATLAB for each of the five edge-support conditions. The *nlinfit* function produces a vector of parameters and the residuals when provided the independent and dependent variable arrays ( $Z$ ,  $k_c^Z$ ). In other words, the function returns the fitted responses and an initial guess of the parameters. See Appendix A for the function files used in conjunction with the *nlinfit* function for each edge-support condition.

The coefficient of determination ( $R^2$ ) is calculated for each case to show how well the regression results matched the CU-FSM data. These values are calculated according to

$$R^2 = 1 - \frac{\sum(y_i - \bar{y})^2}{\sum(y_i - f_i)^2} = 1 - \frac{\sum(k_{c,i}^{Z,CU-FSM} - \bar{k}_c^{Z,CU-FSM})^2}{\sum(k_{c,i}^{Z,CU-FSM} - \bar{k}_c^{Z,MATLAB})^2} \quad (\text{Eq. 7})$$

where  $y_i$  is the calculated  $k_c^Z$  from the CU-FSM data at a specific value of  $Z$ ,  $\bar{y}$  is the average of CU-FSM buckling coefficients for all  $Z$ -values, and  $f_i$  is the buckling coefficient as calculated from Eq. 5 for each of the corresponding  $Z$ -values.

Given the buckling coefficient values for each curvature parameter, the critical elastic buckling stress ratio can then be used to normalize the CU-FSM data for each edge-support condition. The critical buckling stress ratio  $\sigma_{cr}^Z / \sigma_{cr}^{plate}$  can be calculated by

$$\frac{\sigma_{cr}^Z}{\sigma_{cr}^{plate}} = \frac{k_{cr}^Z}{k_{cr}^{plate}} \quad (\text{Eq. 8})$$

where the flat plate is approximated by the results from  $Z = 0.01$ . Providing the data in terms of normalized ratios generates curves for both the nonlinear regression results and CU-FSM results with an intercept at one, allowing for a comparison across all edge-support conditions.

## 4. MODELS AND RESULTS

### 4.1 Edge-support Conditions

#### 4.1.1 Pin-Pin

The simply supported edge-support conditions are restrained in the x- and z- directions at both end nodes. Buckling stresses are found through CU-FSM analysis at each  $Z$ -value. Using the critical buckling stress ratio and Eq. 4, the curved plate buckling coefficient,  $k_c^Z$ , is calculated for each of the twenty selected curvature parameters. When plotted against  $Z$ , the buckling coefficients behaved according to Eq. 9

$$k_c^Z = \frac{k_c^{plate}}{2} (1 + \sqrt{1 + BZ^2}) \quad (\text{Eq. 9})$$

with a  $k_c^{plate}$  of 4.0 (Figure 3). Based on this observation, the *nlinfit* function in MATLAB is used to determine the value of the parameter,  $B$ . Providing the CU-FSM results for  $Z$  and  $k_c^Z$  as input and using an initial guess at  $B$ , the nonlinear regression analysis yielded a value of  $B=0.109$ . This value is similar to the equivalent parameters in Redshaw's and Stowell's equations, respectfully

$$B_{Redshaw} = \frac{12(1 - \nu^2)}{\pi^4} = 0.1098$$

$$B_{Stowell} = \frac{48(1 - \nu^2)}{\pi^4 (k_c^{plate})^2} = 0.1097$$

which is expected because these equations were originally developed for the pin-pin edge-support condition model (LeTran & Davaine, 2011).

Figure 13 shows the buckled shape of sections with three different curvature parameters. A three-dimensional view is also given to aid in both the understanding of the behavior of the whole plate when subject to a uniform compressive stress and the visualization of other results shown.

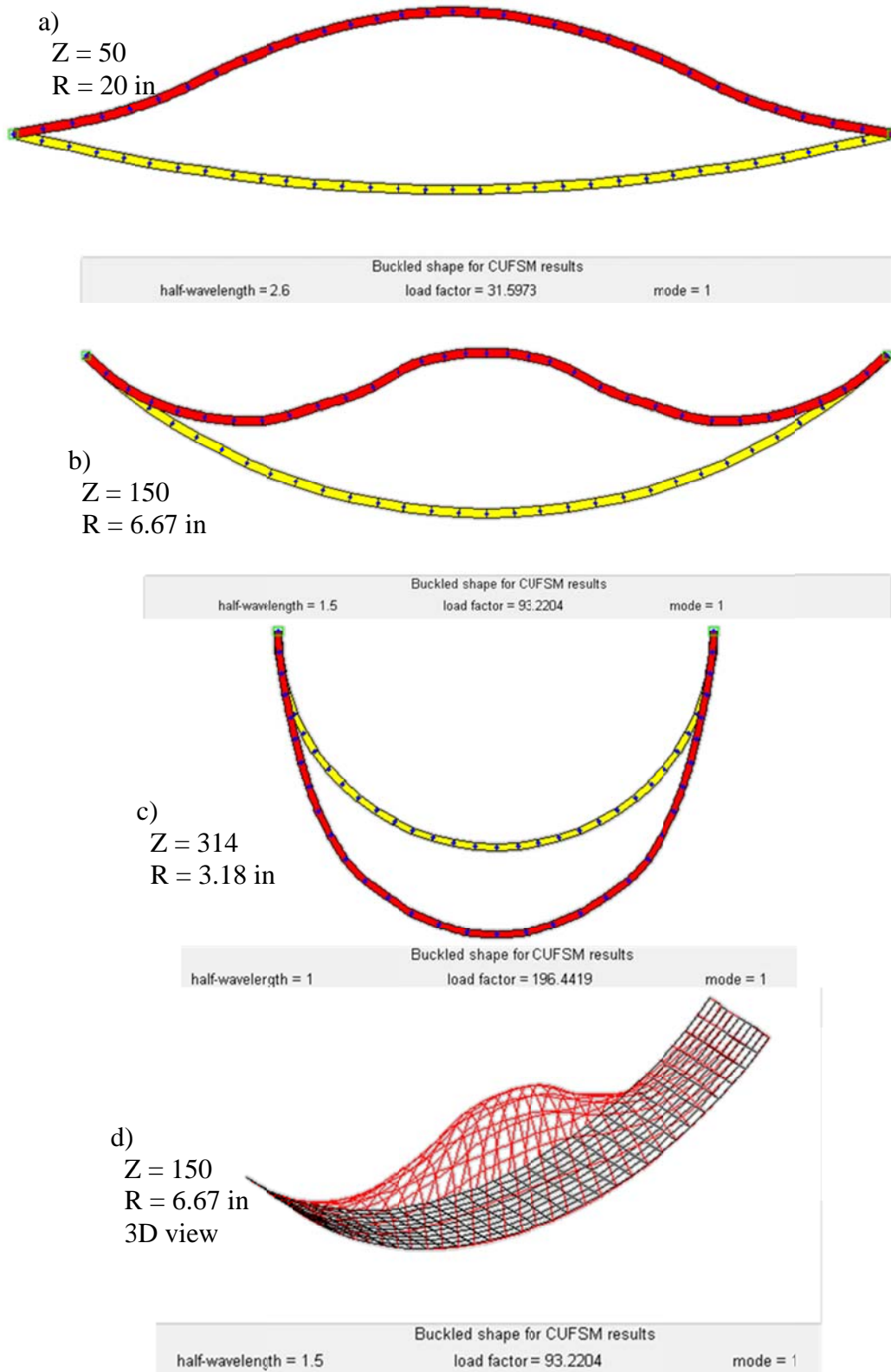


**Figure 13.** Buckled shapes for the pin-pin condition at a range of curvature parameters

Table 3 includes the critical buckling stress and wavelength values obtained through CU-FSM analysis, the buckling coefficients as calculated from Eq. 4, and the values for the buckling coefficient from the nonlinear regression analysis performed using MATLAB. The parameter,  $B$ , used in Eq. 9 is shown along with the coefficient of determination ( $R^2$ ) comparing the CU-FSM results to the generated equation.

**Table 3.** CU-FSM results with output from the nonlinear regression for the pin-pin edge-support condition case

Curvature Parameter, $Z$	$B_{pin-pin} = 0.109$		$R^2 = 0.9998$	
	Critical Buckling Stress (ksi), $\sigma_{cr, CU-FSM}$	Half Wavelength (in)	Buckling Coefficient from CU-FSM, $k_{c,CU-FSM}^Z$	Buckling Coefficient from MATLAB, $k_{c,MATLAB}^Z$
0.01	3.7288	10	4.000	4.000
0.5	3.8106	9.8	4.088	4.027
1	3.7927	9.9	4.069	4.106
2	4.2167	8.9	4.523	4.397
5	5.1463	7.6	5.521	5.860
10	8.0892	5.5	8.677	8.899
20	13.562	4.1	14.55	15.36
30	19.473	3.3	20.89	21.91
34.9	22.5	3.1	24.14	25.13
35	22.5	3.1	24.14	25.20
50	31.5973	2.6	33.90	35.08
100	62.215	1.8	66.74	68.06
120	74.9218	1.6	80.37	81.26
135	83.9449	1.5	90.05	91.16
150	93.2204	1.5	100.0	101.1
157	97.6299	1.4	104.7	105.7
200	124.7926	1.3	133.9	134.1
250	156.3662	1.1	167.7	167.1
300	188.0642	1	201.7	200.1
314	196.4419	1	210.2	209.3

The coefficient of determination  $R^2$  is close to unity indicating a strong correlation between the CU-FSM data and the derived equation. For the pin-pin edge-support condition case, this generated equation is

$$k_{c,pin-pin}^Z = \frac{4}{2}(1 + \sqrt{0.109Z^2}) \quad (\text{Eq. 10})$$

and the goodness of fit can be observed in Figure 14. Note the intercept is at  $k_{cr}=4$ , which is the flat plate buckling coefficient for this edge-support condition.

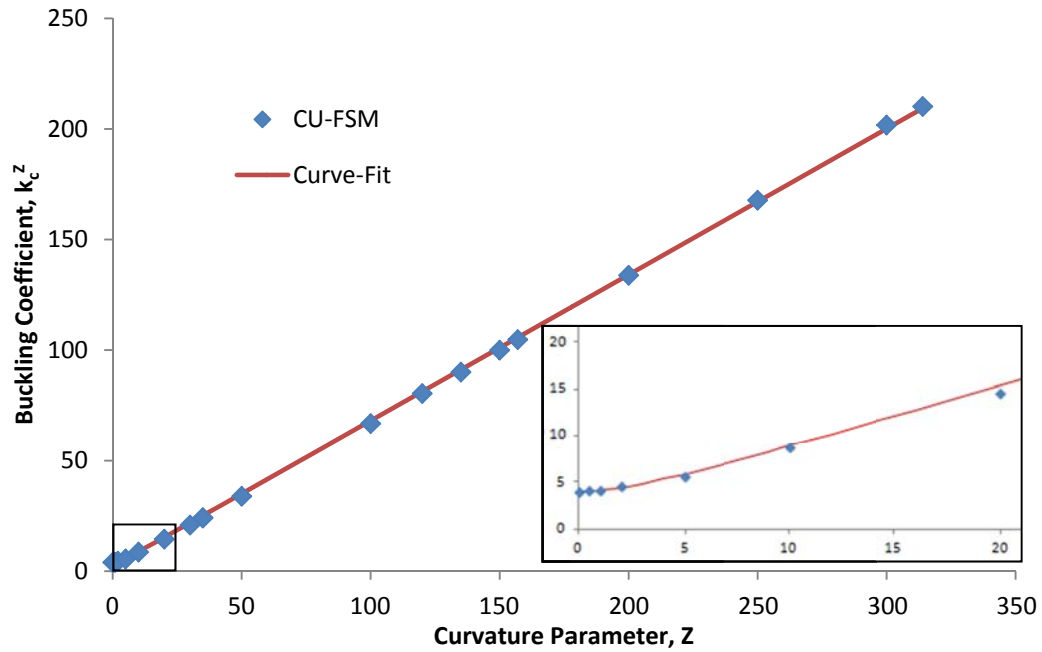


**Figure 14.** Plot of CU-FSM data points and the nonlinear regression model from MATLAB for the pin-pin edge-support conditions with the inset showing the intercept at the flat plate buckling coefficient.

Figure 15 shows a plot of the critical buckling stress ratio versus the curvature parameter. It can be observed that in all cases as the curvature parameter increases, the critical buckling stress ratio increases as well.

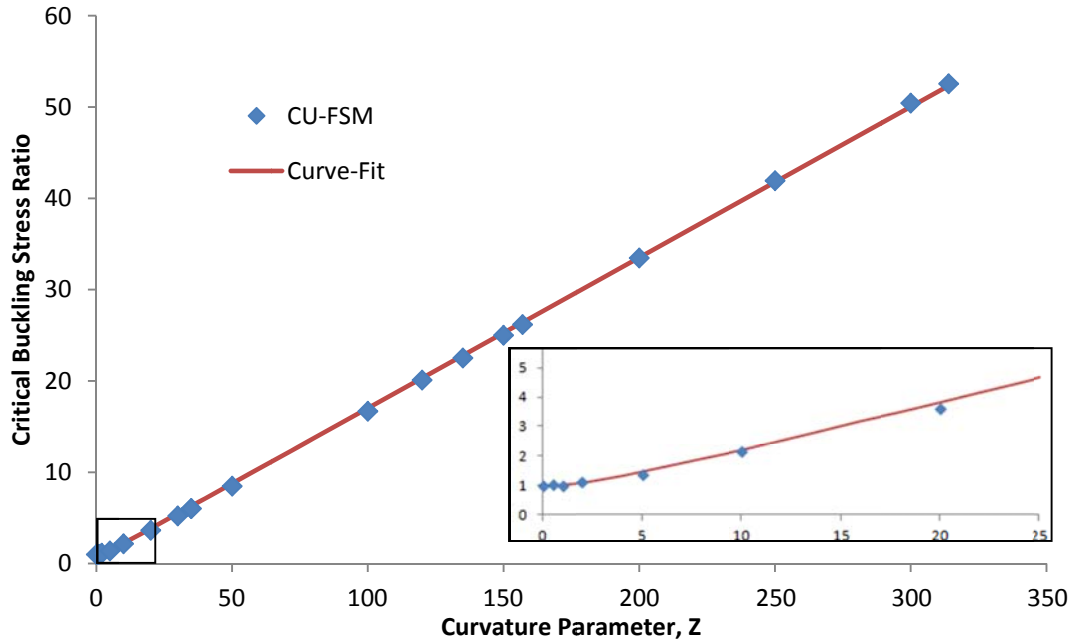


**Figure 15.** Critical buckling stress ratio for the pin-pin condition with inset showing the intercept at 1

#### 4.1.2 Pin-Fixed

The pin-fixed edge-support conditions are restrained in the x- and z-directions on both edges with a rotational restrained on one edge. Elastic buckling stresses are found through CU-FSM analysis at each Z-value. Using the critical buckling stress ratio and Eq. 4, the curved plate buckling coefficient  $k_c^Z$  is calculated for each curvature parameter. When plotted against Z, the buckling coefficients behaved according to Eq. 11

$$k_c^Z = \frac{k_c^{plate}}{2} (1 + \sqrt{1 + BZ^2}) \quad (\text{Eq. 11})$$

with  $k_c^{plate} = 5.42$  (Figure 3). Based on this observation, the *nlinfit* function in MATLAB is used to determine the value of the parameter, B. With input including the CU-FSM



results for  $Z$  and  $k_c^Z$  and an initial guess at  $B$ , the nonlinear regression analysis yielded a value of  $B=0.0587$ . This value is significantly different when compared to the equivalent parameters in Redshaw's and Stowell's equations of

$$B_{Redshaw} = \frac{12(1 - \nu^2)}{\pi^4} = 0.1098$$

$$B_{Stowell} = \frac{48(1 - \nu^2)}{\pi^4(k_c^{plate})^2} = 0.0149$$

This indicates an alternative parameter is needed, thereby validating the purpose of this study and that by LeTran and Davaine (2011).

Figure 16 shows the buckled shape of sections with three different curvature parameters and a three-dimensional view. Table 4 includes the numerical results for this edge-support condition.

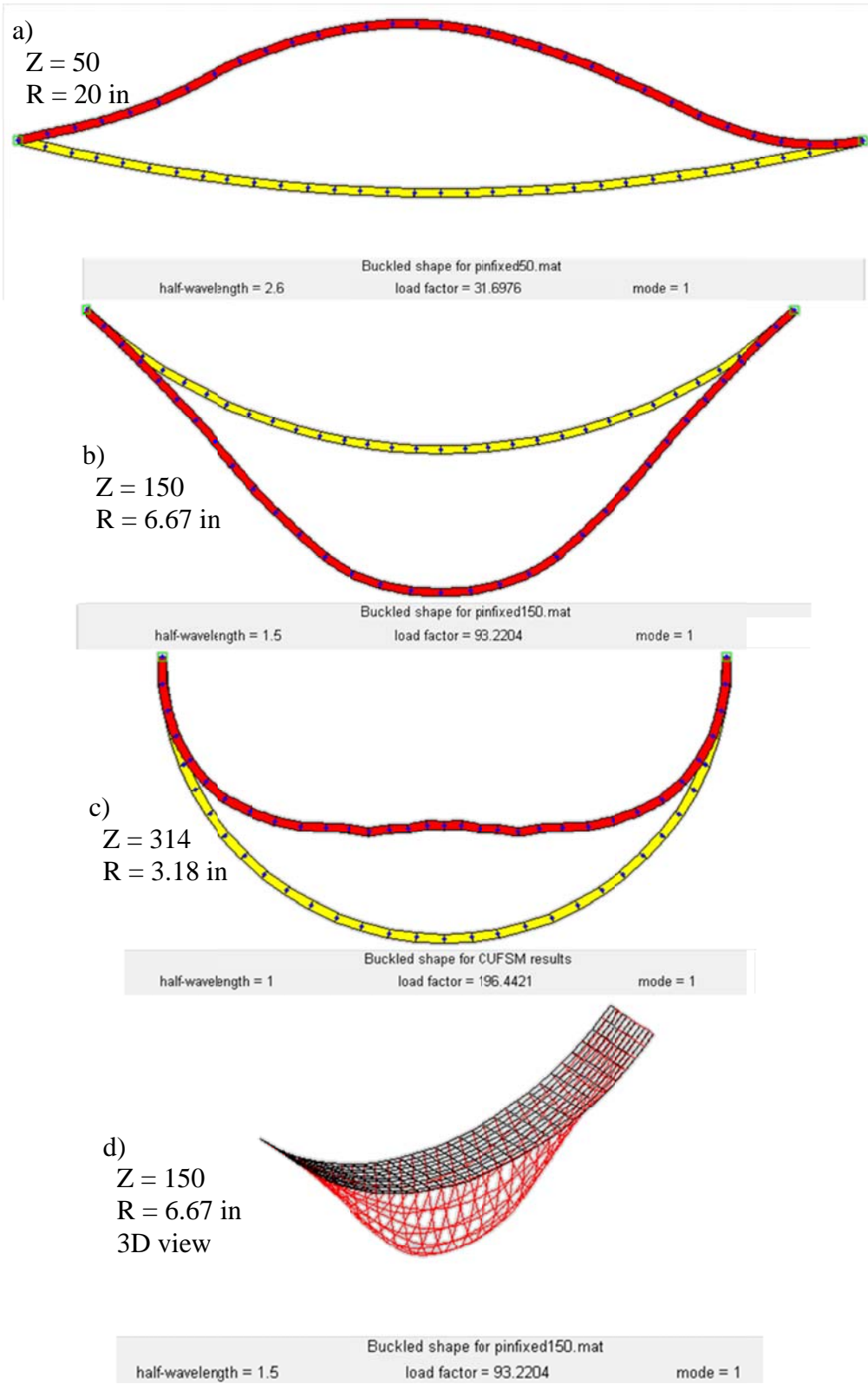


**Figure 16.** Buckled shapes for the pin-fixed condition at a range of curvature parameters

**Table 4.** CU-FSM results with output from the nonlinear regression for the pin-fixed edge-support condition case

	$B_{pin-fixed} = 0.0587$		$R^2 = 0.9997$	
Curvature Parameter, $Z$	Critical Buckling Stress (ksi), $\sigma_{cr, CU-FSM}$	Half Wavelength (in)	Buckling Coefficient from CU-FSM, $k_{c,CU-FSM}^Z$	Buckling Coefficient from MATLAB, $k_{c,MATLAB}^Z$
0.01	5.0432	8	5.410	5.420
0.5	5.0727	7.9	5.442	5.440
1	5.11	7.9	5.482	5.498
2	5.2406	7.7	5.622	5.721
5	6.1209	6.9	6.566	6.967
10	8.3569	5.9	8.965	9.813
20	13.8694	4.1	14.878	16.118
30	19.5937	3.4	21.019	22.593
34.9	22.5221	3.1	24.160	25.784
35	22.6863	3.1	24.336	25.850
50	31.6976	2.6	33.952	35.651
100	62.3161	1.8	66.848	68.424
120	74.7024	1.6	80.135	81.546
135	84.4738	1.5	90.617	91.390
150	93.2204	1.5	99.972	101.234
157	97.7094	1.4	104.815	105.829
200	124.6699	1.3	133.736	134.054
250	156.2851	1.1	167.650	166.878
300	187.2006	1.3	200.814	199.703
314	196.4421	1	209.197	208.894

Once again, the coefficient of determination is close to unity indicating a strong correlation between the CU-FSM data and the derived equation. For the fixed-pin edge-support condition case, this generated equation is

$$k_{c, fixed-pin}^Z = \frac{5.42}{2} (1 + \sqrt{0.0587Z^2}) \quad (\text{Eq. 12})$$

and the goodness of fit can be observed in Figure 17. Note the intercept is at  $k_{cr}=5.42$ , which is the flat plate buckling coefficient for this edge-support condition. As shown in Figure 18, an increase in the curvature parameter results in an increase in the critical buckling stress ratio.

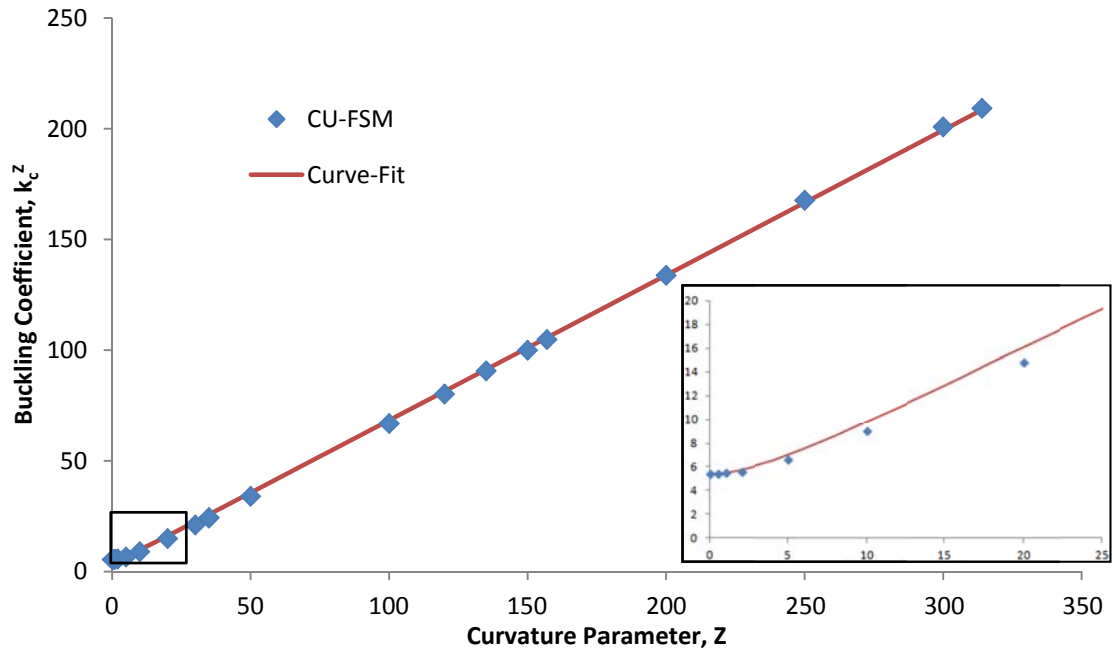


**Figure 17.** Plot of CU-FSM data points and the nonlinear regression model from MATLAB for the fixed-pin edge-support conditions with the inset showing the intercept at the flat plate buckling coefficient

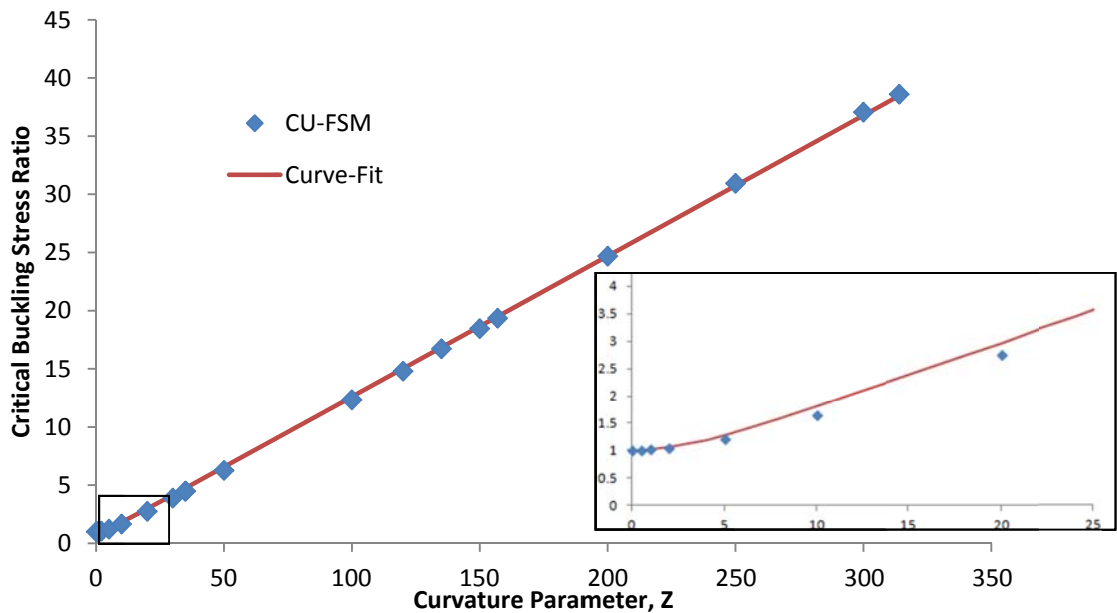


**Figure 18.** Critical buckling stress ratio for the fixed-pin condition with inset showing the intercept at 1

### 4.1.3 Fixed-Fixed

The fixed-fixed edge-support conditions are restrained longitudinally in the x- and z-directions and rotationally on both edges. Using the same approach as described above, the equation derived for computing the curved plate buckling coefficient for the fixed-fixed case is

$$k_{c, fixed-fixed}^Z = \frac{6.97}{2} (1 + \sqrt{0.0349Z^2}) \quad (\text{Eq. 13})$$

with 6.97 equaling the flat plate coefficient  $k_c^{plate}$  (Figure 3). The factor 0.0349 is again different from that obtained by Redshaw's and Stowell's equations

$$B_{Redshaw} = \frac{12(1 - \nu^2)}{\pi^4} = 0.1098$$

$$B_{Stowell} = \frac{48(1 - \nu^2)}{\pi^4 (k_c^{plate})^2} = 0.00904$$

Figure 19 shows the buckling modes for three Z-values and Table 5 provides critical buckling stresses, wavelengths, and the values for the buckling coefficient from the nonlinear regression analysis performed using MATLAB.

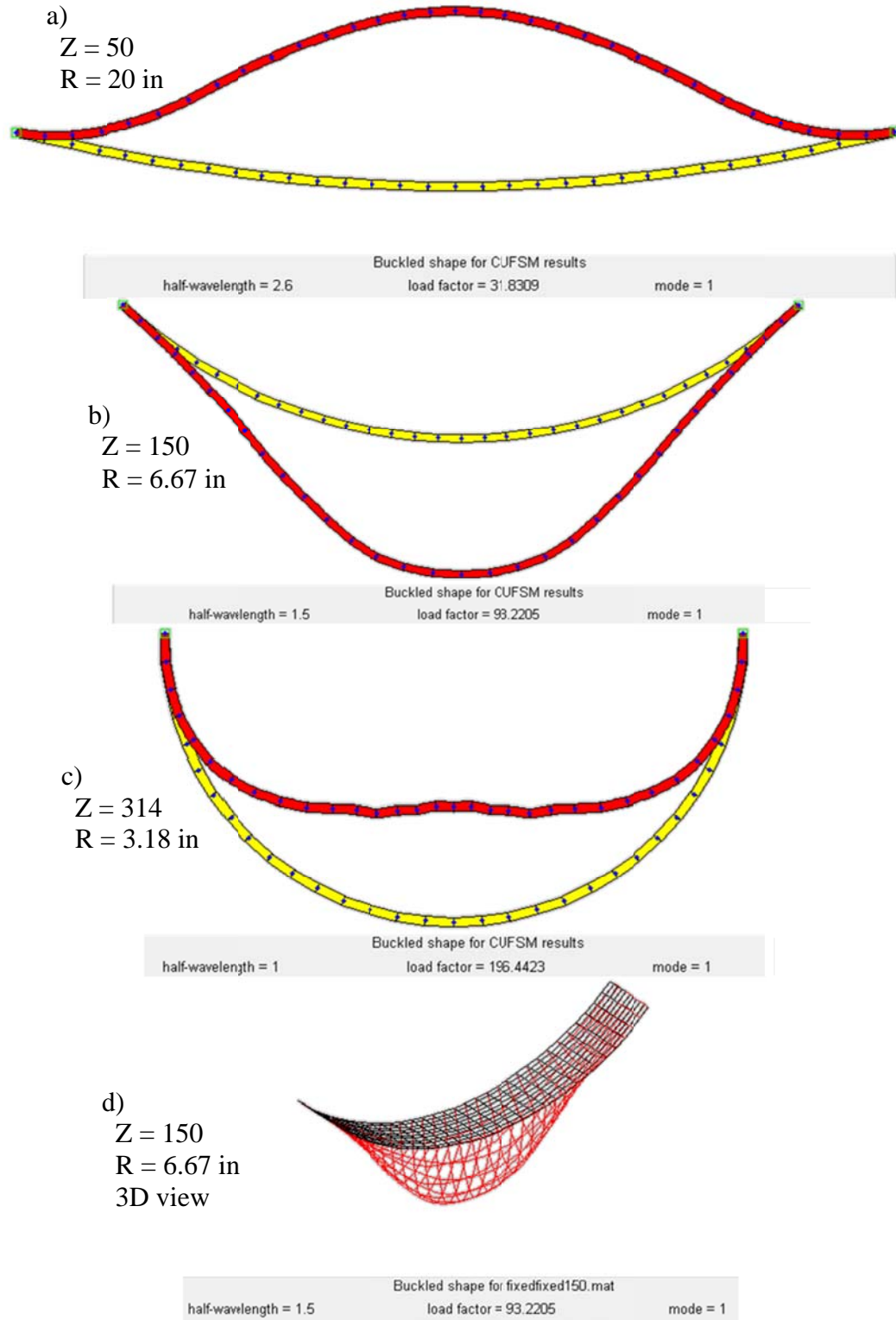


**Figure 19.** Buckled shapes for the fixed-fixed condition at a range of curvature parameters

**Table 5.** CU-FSM results with output from the nonlinear regression for the fixed-fixed edge-support condition case

	$B_{fixed-fixed} = 0.0349$		$R^2 = 0.9995$	
<b>Curvature Parameter, <math>Z</math></b>	<b>Critical Buckling Stress (ksi), <math>\sigma_{cr, CU-FSM}</math></b>	<b>Half Wavelength (in)</b>	<b>Buckling Coefficient from CU-FSM, <math>k_{c,CU-FSM}^Z</math></b>	<b>Buckling Coefficient from MATLAB, <math>k_{c,MATLAB}^Z</math></b>
0.01	6.4984	6.6	6.970	6.970
0.5	6.5256	6.6	6.999	6.985
1	6.5445	6.6	7.019	7.030
2	6.6192	6.5	7.100	7.205
5	7.2624	6.1	7.789	8.254
10	9.0214	5.3	9.676	10.870
20	14.2523	4.1	15.287	16.964
30	19.8264	3.4	21.265	23.325
34.9	22.7002	3.1	24.348	26.472
35	22.883	3.1	24.544	26.537
50	31.8309	2.6	34.040	36.224
100	62.3228	1.8	66.846	68.683
120	74.7301	1.6	80.153	81.689
135	84.512	1.5	90.645	91.446
150	93.2205	1.5	99.963	101.205
157	97.7152	1.4	104.807	105.760
200	124.6852	1.3	133.734	133.742
250	156.3013	1.1	167.644	166.285
300	187.2535	1.3	200.843	198.832
314	196.4423	1	209.198	207.945

Figure 20 illustrates the goodness of fit of the derived equation and as observed in Figure 21 an increase in the curvature parameter once again results in an increase in the critical buckling stress ratio.

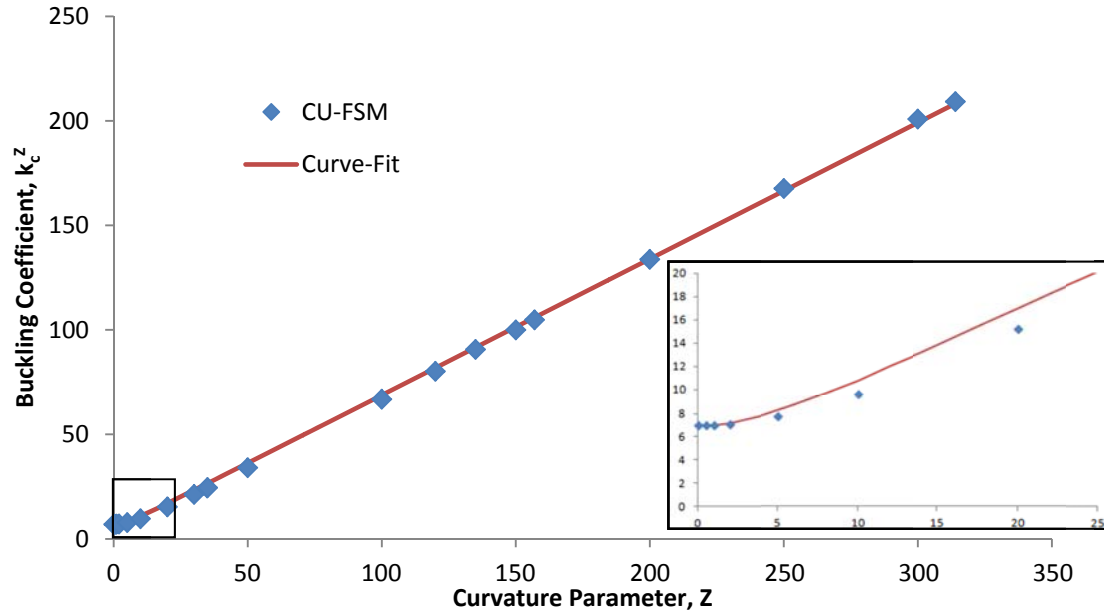


**Figure 20.** Plot of CU-FSM data points and the nonlinear regression model from MATLAB for the fixed-fixed edge-support conditions with the inset showing the intercept at the flat plate buckling coefficient

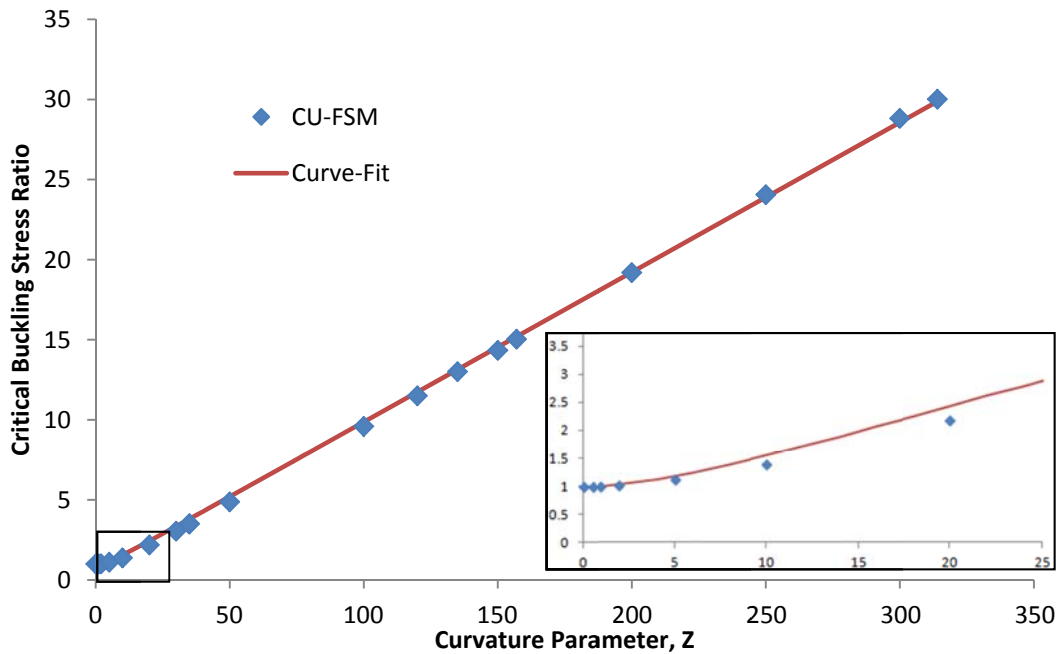


**Figure 21.** Critical buckling stress ratio for the fixed-fixed condition with inset showing the intercept at 1



#### 4.1.4 Fixed-Free

The fixed-free edge-support conditions are restrained longitudinally in the x- and z-directions and rotationally on one edge and completely unrestrained along the other edge. For this case, the plate buckling coefficient may be estimated from

$$k_{c, fixed-free}^Z = \frac{1.277}{2} (1 + \sqrt{0.0201Z^2}) \quad (\text{Eq. 14})$$

with the parameter  $B = 0.0201$  being significantly different than Redshaw's 0.1098 and Stowell's 0.2693. Using a similar format to the cases presented above the key results are provided in Figures 22, 23, and 24 and Table 6.

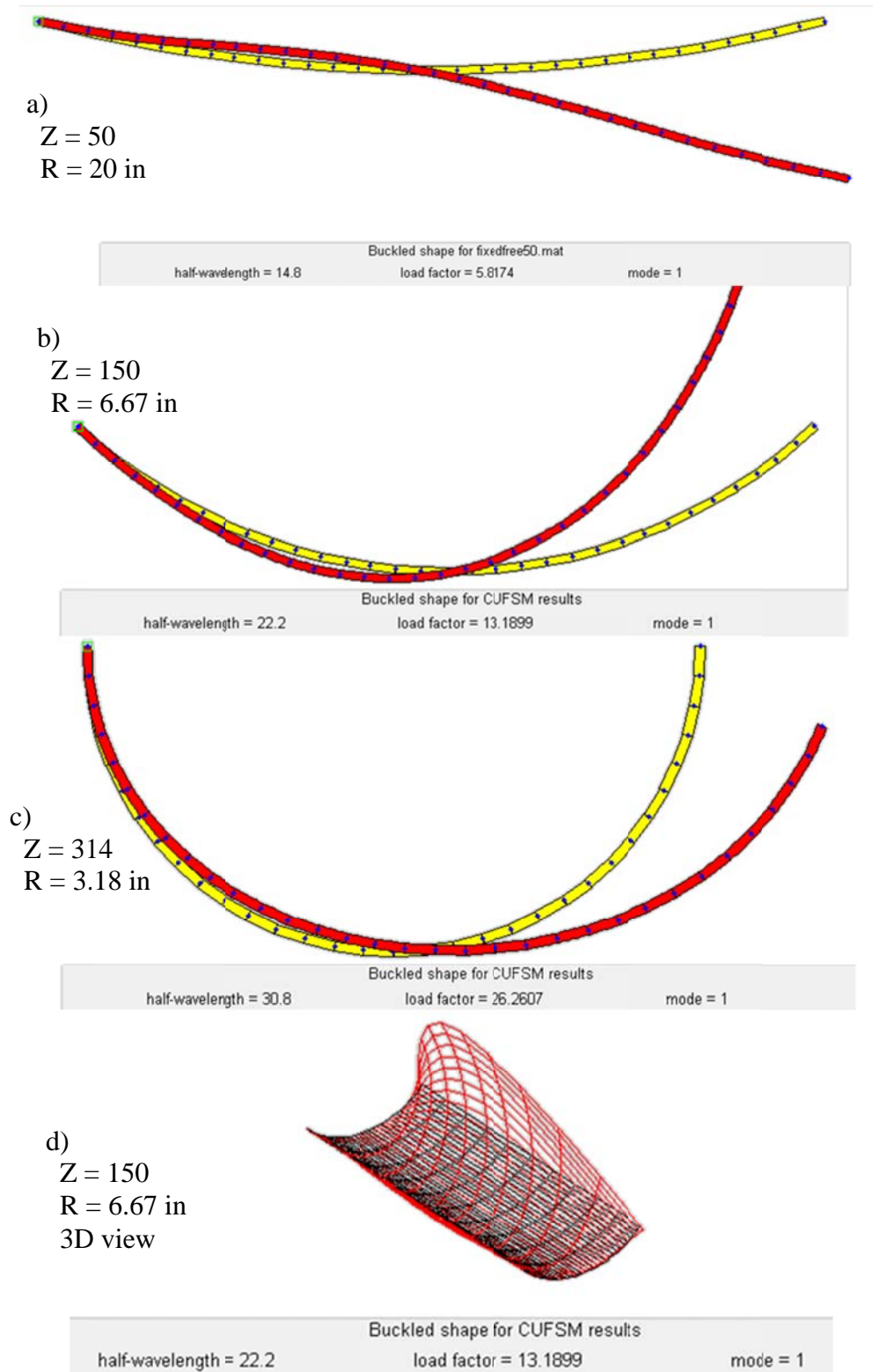


**Figure 22.** Buckled shapes for the fixed-free condition at a range of curvature parameters

**Table 6.** CU-FSM results with output from the nonlinear regression for the fixed-free edge-support condition case

	$B_{fixed-free} = 0.0201$		$R^2 = 0.9952$	
<b>Curvature Parameter, <math>Z</math></b>	<b>Critical Buckling Stress (ksi), <math>\sigma_{cr, CU-FSM}</math></b>	<b>Half Wavelength (in)</b>	<b>Buckling Coefficient from CU-FSM, <math>k_{c,CU-FSM}^Z</math></b>	<b>Buckling Coefficient from MATLAB, <math>k_{c,MATLAB}^Z</math></b>
0.01	1.165	16.4	1.277	1.277
0.5	1.1688	16.4	1.281	1.279
1	1.1738	16.5	1.287	1.283
2	1.1901	16.6	1.305	1.302
5	1.337	17.6	1.466	1.421
10	1.7616	20.7	1.931	1.746
20	2.9144	28.7	3.195	2.558
30	4.0771	35.1	4.469	3.428
34.9	4.6416	37.8	5.088	3.862
35	4.6601	14	5.108	3.871
50	5.8174	14.8	6.361	5.209
100	9.5329	18.9	10.449	9.713
120	10.8655	20	11.910	11.520
135	11.9208	21	13.067	12.876
150	13.1899	22.2	14.458	14.232
157	13.6911	22.6	15.007	14.865
200	16.8934	25.1	18.517	18.754
250	20.8061	27.5	22.806	23.278
300	24.9831	30.1	27.385	27.803
314	26.2607	30.8	28.785	29.070

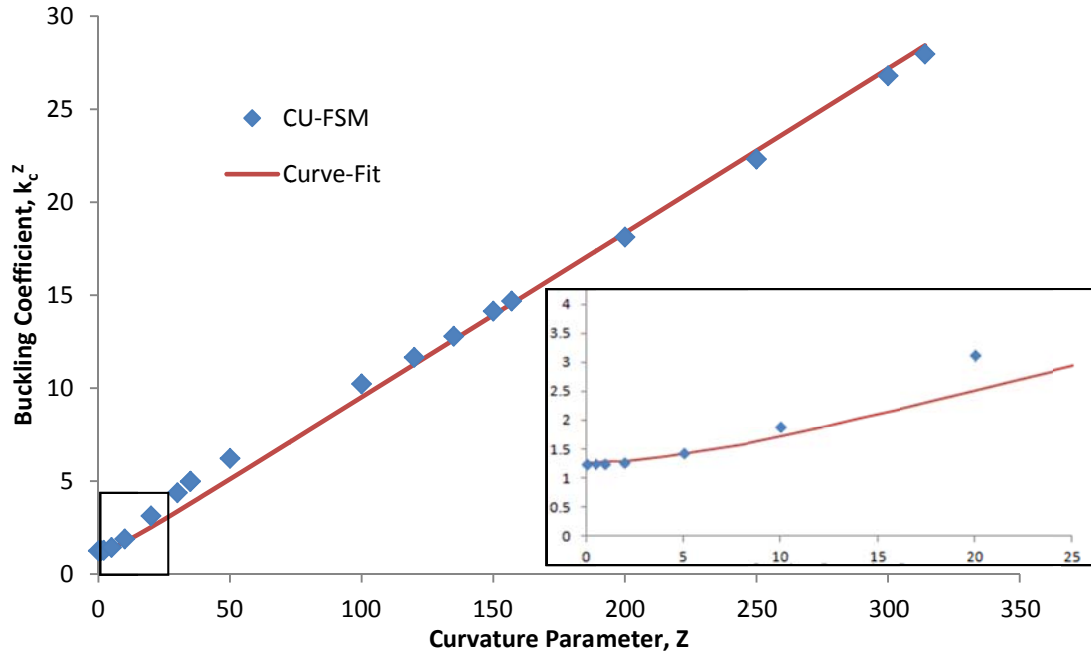


**Figure 23.** Plot of CU-FSM data points and the nonlinear regression model from MATLAB for the fixed-free edge-support conditions with the inset showing the intercept at the flat plate buckling coefficient

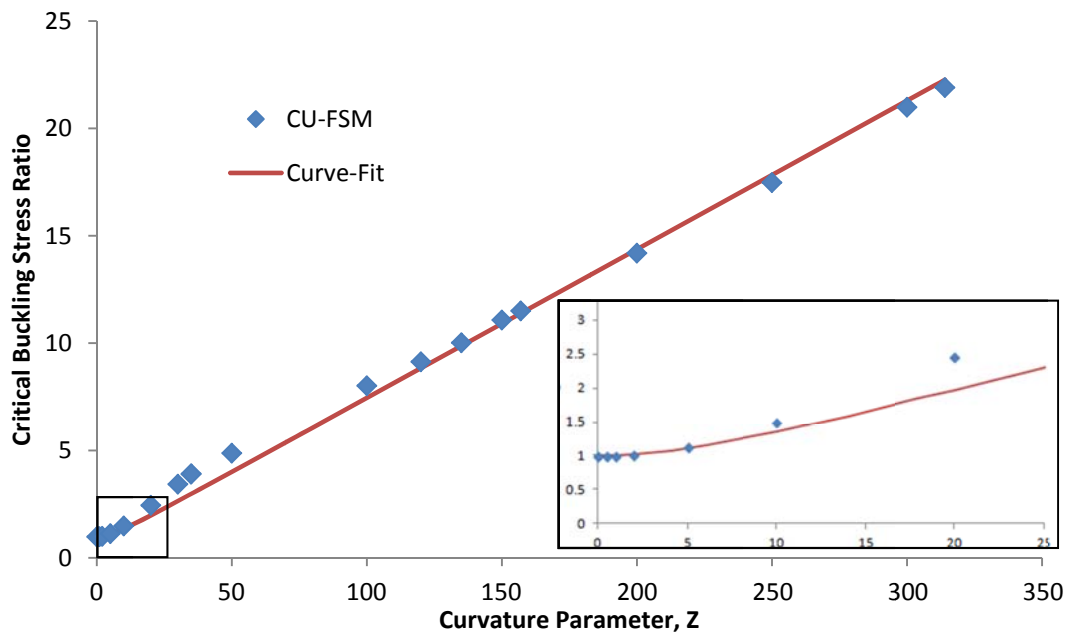


**Figure 24.** Critical buckling stress ratio for the fixed-free condition with inset showing the intercept at 1

#### 4.1.5 Pin-Free

The pin-free edge-support conditions are restrained longitudinally in the x- and z- directions on one edge and completely unrestrained on the other edge. With a consistent procedure to the previous edge-support conditions, the derived plate buckling coefficient equation is

$$k_{c,pin-free}^Z = \frac{0.425}{2} (1 + \sqrt{0.1737Z^2}) \quad (\text{Eq. 15})$$

where the value  $B=0.1737$  is different than the values calculated through Redshaw's ( $B=0.1098$ ) and Stowell's ( $B=2.431$ ) equations. Following a similar format to the edge-support conditions presented above, the results for the pin-free condition are found in Figures 25, 26, and 26 and Table 7.

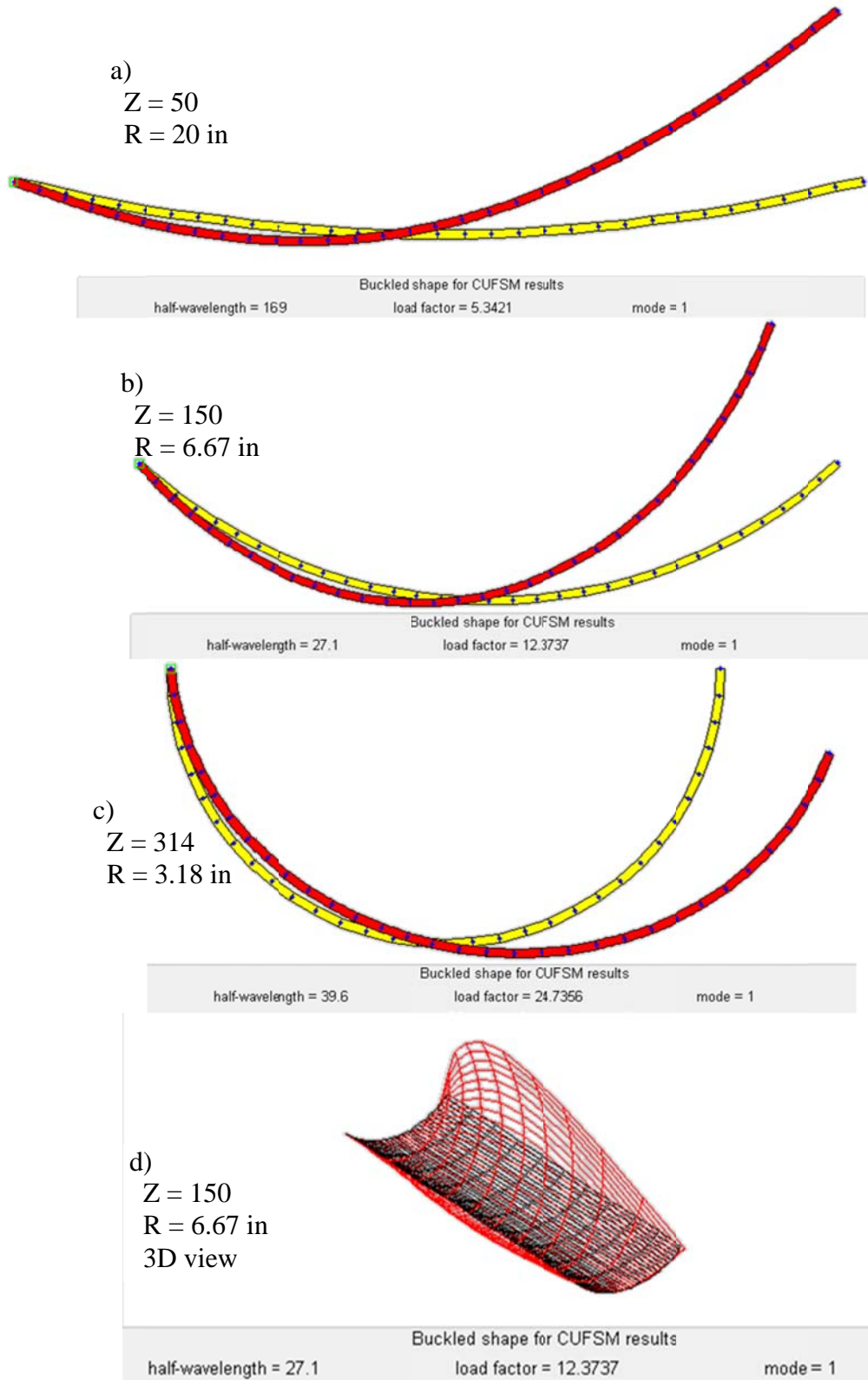


**Figure 25.** Buckled shapes for the pin-free condition at a range of curvature parameters

**Table 7.** CU-FSM results with output from the nonlinear regression for the pin-free edge-support condition case

	$B_{pin-free} = 0.1737$		$R^2 = 0.9911$	
<b>Curvature Parameter, <math>Z</math></b>	<b>Critical Buckling Stress (ksi), <math>\sigma_{cr, CU-FSM}</math></b>	<b>Half Wavelength (in)</b>	<b>Buckling Coefficient from CU-FSM, <math>k_{c,CU-FSM}^Z</math></b>	<b>Buckling Coefficient from MATLAB, <math>k_{c,MATLAB}^Z</math></b>
0.01	0.38045	345	0.425	0.425
0.5	0.38001	535	0.425	0.430
1	0.37986	731	0.424	0.443
2	0.37989	690	0.424	0.489
5	0.3798	834	0.424	0.704
10	0.38076	1097	0.425	1.123
20	0.38234	1295	0.427	1.996
30	3.9918	15.2	4.459	2.878
34.9	4.2998	15.4	4.803	3.311
35	4.2933	15.2	4.796	3.320
50	5.3421	16.9	5.946	4.646
100	8.8551	22.5	9.892	9.071
120	10.1664	24.2	11.357	10.842
135	11.1874	25.5	12.497	12.171
150	12.3737	27.1	13.823	13.499
157	12.8493	27.6	14.354	14.119
200	15.9141	31	17.778	17.927
250	19.6685	34.8	21.972	22.355
300	23.5619	38.6	26.321	26.783
314	24.7396	39.6	27.444	28.023

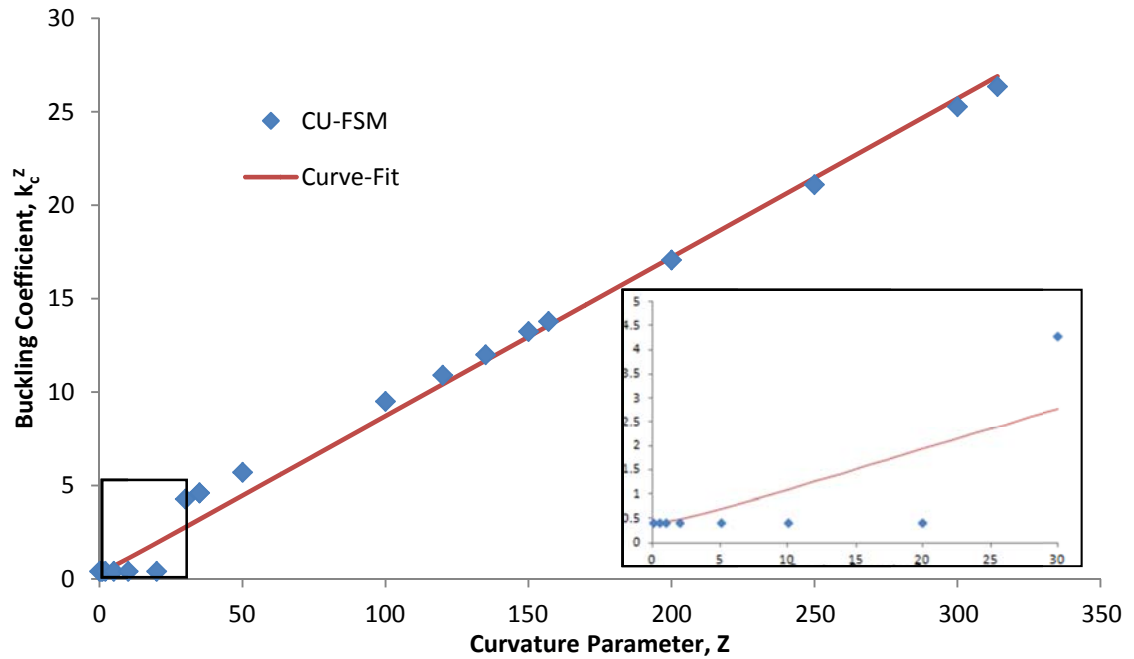


**Figure 26.** Plot of CU-FSM data points and the nonlinear regression model from MATLAB for the pin-free edge-support conditions with the inset showing the intercept at the flat plate buckling coefficient

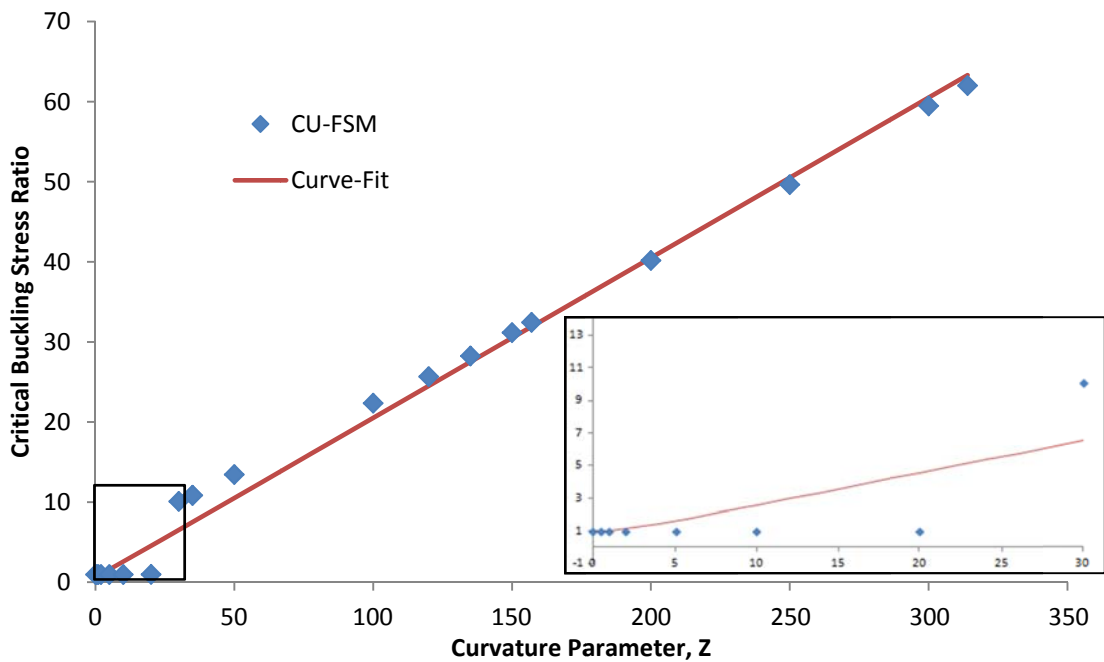


**Figure 27.** Critical buckling stress ratio for the fixed-fixed condition with inset showing the intercept at 1



## 4.2 Summary of Results

In each edge-support condition case presented above, it can be observed that the critical buckling stress ratios increase with the curvature parameter. This indicates, for sections with the same  $b/t$  ratio, the critical buckling stress will increase as the radius of the section decreases. Table 8 shows the calculated parameter,  $B$ , used to fit the CU-FSM data from each edge-support condition in the form

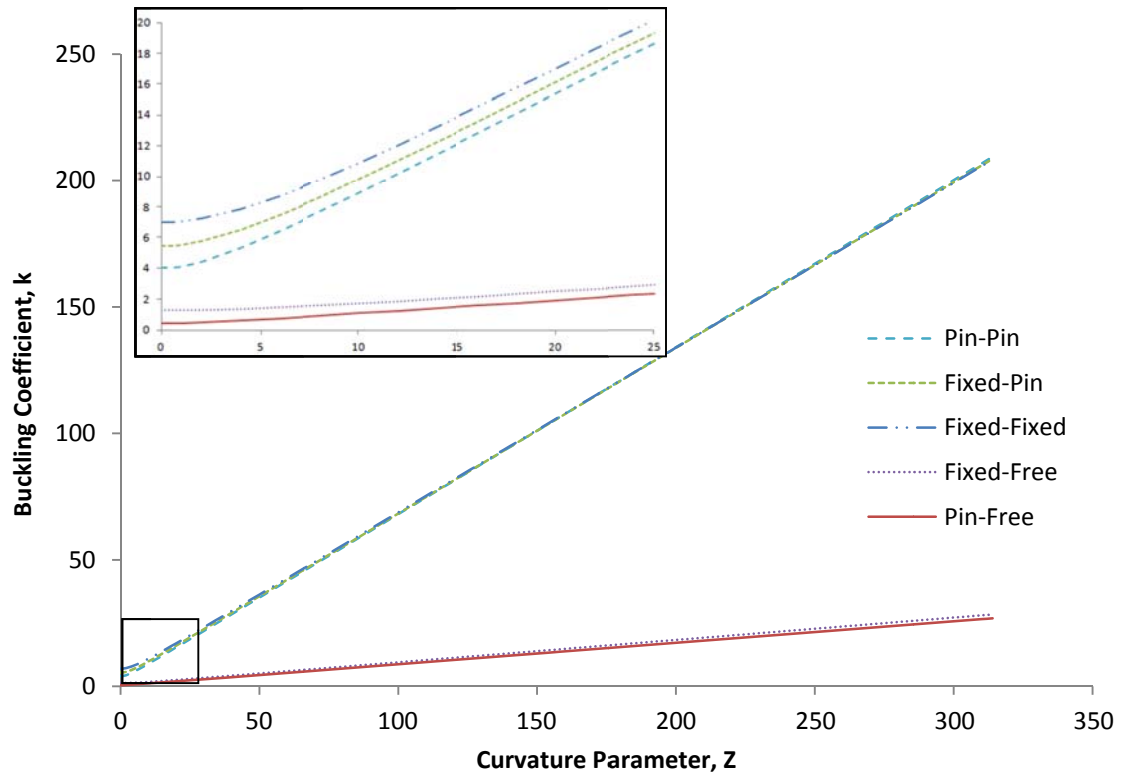
$$k_c^Z = \frac{k_c^{plate}}{2} (1 + \sqrt{1 + BZ^2}) \quad (\text{Eq.16})$$

as well as the coefficient of determination,  $R^2$ , for each case. Note that all of the  $R^2$  values are close to unity, indicating the nonlinear regression analysis yielded an equation that accurately represents the data points generated through CU-FSM analysis.

**Table 8.** Summary of results of nonlinear regression analysis

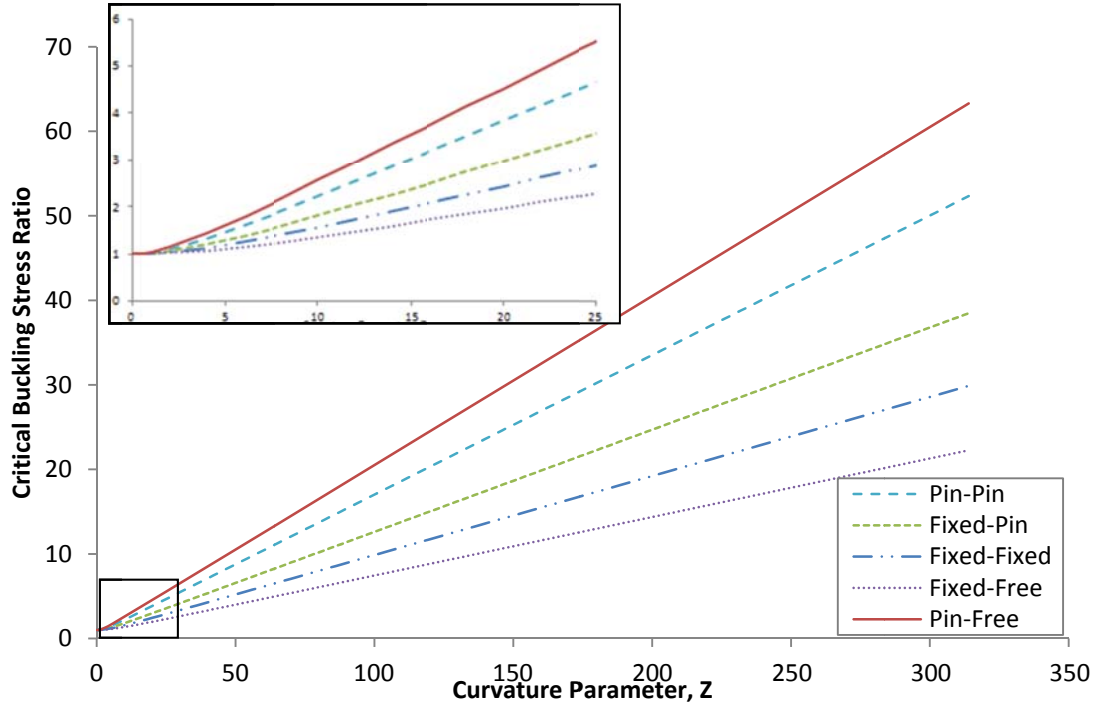
Edge-support Condition	Plate Buckling Coefficient, $k_c^{plate}$	Calculated Parameter, $B$	Coefficient of Determination, $R^2$
Pin-Pin	4.0	0.1090	0.99983
Pin-Fixed	5.42	0.0587	0.99975
Fixed-Fixed	6.97	0.0349	0.99956
Fixed-Free	1.277	0.0201	0.99528
Pin-Free	0.425	0.1737	0.99118

Figure 28 shows the buckling coefficients obtained from regression analysis for all five edge-support conditions over a wide range of curvature  $Z$ -parameters. It can be seen that each curve intercepts the  $y$ -axis at the plate buckling coefficient value for that edge-support condition.



**Figure 28.** Buckling coefficients from nonlinear regression analysis versus curvature parameter,  $Z$  for each edge-support condition considered in this study

Figure 29 shows the relationship between the curvature parameter,  $Z$ , and the critical buckling stress ratio,  $\sigma_{cr}^Z / \sigma_{cr}^{plate}$ , for each of the five edge-support condition cases considered. As expected, the shape of the curves is similar to that of the ratio of buckling coefficients provided in Figure 28. This further confirms the assumption that the critical buckling strength ratios can also be fit with the same curve as the buckling coefficients.



**Figure 29.** Critical buckling stress ratios versus curvature parameter for all five edge-support conditions

## 5. EXAMPLES

Two examples are presented to show the similarities between the elastic critical buckling stresses of a curved plate as determined by CU-FSM analysis and by the use of the equation developed in this study

$$k_c^Z = \frac{k_c^{plate}}{2} (1 + \sqrt{1 + BZ^2}) \quad (\text{Eq. 17})$$

$$\sigma_c^Z = k_c^Z \sigma_E \quad (\text{Eq. 18})$$

### 5.1 Example 1

Consider a section where the thickness is  $t = 0.09$  inches,  $b = 3$  inches, and  $R = 1.5$  inches with (a) pin-pin edge-support conditions, (b) pin-free edge-support conditions and (c) fixed-fixed edge-support conditions. Figure 30 shows the shape of this section.

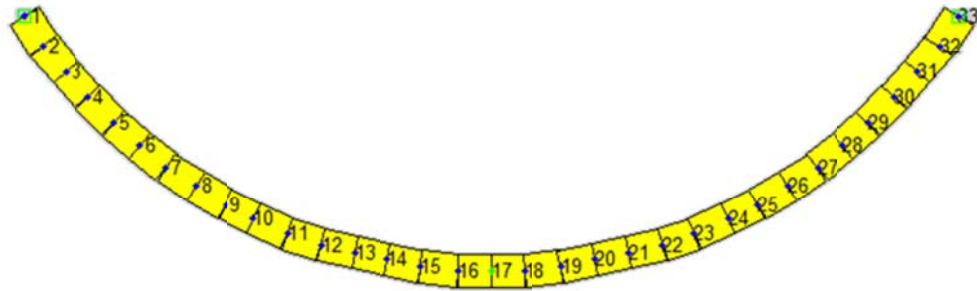


**Figure 30.** Geometry of the section used in Example 1

To use Eq. 17 and Eq. 18, the curvature  $Z$ -parameter and elastic buckling stress with  $k = 1$  must be first calculated.

$$Z = \frac{(3)^2}{1.5 * 0.09} = 66.67$$

$$\sigma_E = \frac{\pi^2 E}{12(1 - \nu^2) \left(\frac{b}{t}\right)^2} = \frac{\pi^2 (10100)}{12(1 - .33^2) \left(\frac{3}{.09}\right)^2} = 8.39 \text{ ksi}$$

Both of these values will be the same for each edge-support condition. The critical buckling stresses will, however, vary with the edge-support conditions.

**(a) Pin-Pin**

The derived equation gives the following critical buckling coefficient and critical buckling stress

$$k_c^Z = \frac{4}{2} \left( 1 + \sqrt{1 + 0.109 * (66.67)^2} \right) = 46.07$$

$$\sigma_c^Z = k_c^Z \sigma_E = 46.07 * 8.39 = 386.53 \text{ ksi}$$

It should be noted that this value is the elastic critical stress and nearly 10 times the yield strength of aluminum. Employing a CU-FSM analysis, the elastic critical buckling stress is computed as

$$\sigma_c^Z = 372.2584 \text{ ksi}$$

The value calculated through the generated equation is within

$$\frac{386.53 - 372.2584}{372.2584} = 3.83\%$$

of the CU-FSM results, indicating a low margin of error.

**(b) Pin-Free**

Following the same procedure as in part (a), the critical buckling coefficient and critical buckling stress were calculated.

$$k_c^Z = \frac{0.425}{2} \left( 1 + \sqrt{1 + .1737 * (66.67)^2} \right) = 6.12$$

$$\sigma_c^Z = k_c^Z \sigma_E = 6.12 * 8.39 = 51.35 \text{ ksi}$$

The calculated elastic critical stress is greater than the yield strength of aluminum. Through CU-FSM analysis, the elastic critical buckling stress was calculated to be

$$\sigma_c^Z = 58.1929 \text{ ksi}$$

resulting in a relatively low margin of error (11.8%) considering the uncertainty in determining a minimum along the buckling curve.

**(c) Fixed-Fixed**

As in the previous examples, the derived values for the critical buckling coefficient and critical buckling stress are

$$k_c^Z = \frac{6.97}{2} \left( 1 + \sqrt{1 + .0349 * (66.67)^2} \right) = 47.03$$

$$\sigma_c^Z = k_c^Z \sigma_E = 47.03 * 8.39 = 394.58 \text{ ksi}$$

with a critical buckling stress nearly 10 times the yield strength of aluminum. CU-FSM analysis yields an elastic critical buckling stress of

$$\sigma_c^Z = 372.3 \text{ ksi}$$

indicating the derived value is within 5.98% error.

## 5.2 Example 2

Now evaluate a section where the thickness is  $t = 0.4$  inches,  $b = 12$  inches, and  $R = 24$  inches with (a) pin-pin edge-support conditions, (b) fixed-free edge-support conditions and (c) pin-fixed edge-support conditions. Figure 31 shows the shape of this section.

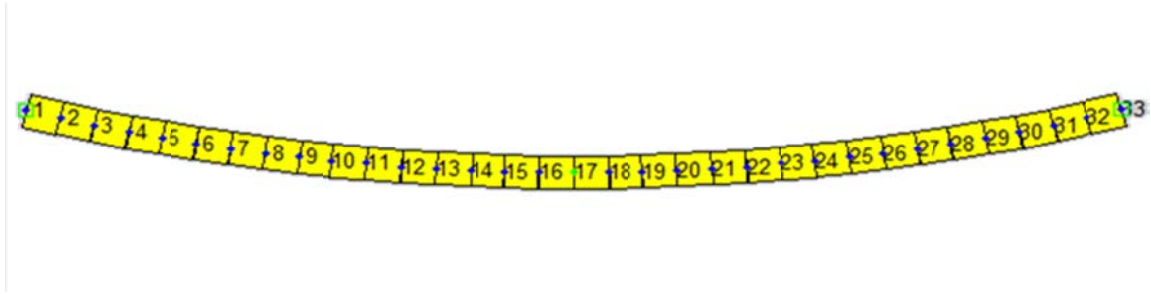


**Figure 31.** Geometry of the section used in Example 2

Again, to use Eq. 17 and Eq. 18, the curvature parameter and Euler buckling stress with  $k=1$  must be calculated.

$$Z = \frac{(12)^2}{24 * 0.4} = 15$$

$$\sigma_E = \frac{\pi^2 E}{12(1 - \nu^2) \left(\frac{b}{t}\right)^2} = \frac{\pi^2 (10100)}{12(1 - .33^2) \left(\frac{12}{0.4}\right)^2} = 10.36 \text{ ksi}$$

These values remain the same for each edge-support condition, whereas the critical buckling stress will vary.

### (a) Pin-Pin

From the derived equation, a critical buckling coefficient and critical buckling stress (in this case, almost triple the yield stress of aluminum) can be calculated.

$$k_c^Z = \frac{4}{2} \left( 1 + \sqrt{1 + 0.109 * (15)^2} \right) = 12.10$$

$$\sigma_c^Z = k_c^Z \sigma_E = 12.10 * 10.36 = 125.36 \text{ ksi}$$

Comparing this value to the results of CU-FSM analysis ( $\sigma_c^Z = 118.1673 \text{ ksi}$ ) the derived equation is within

$$\frac{125.36 - 118.1673}{118.1673} = 6.09\%$$

of the CU-FSM results, indicating a low margin of error.

### (b) Fixed-Free

Using the procedure outlined previously, the critical buckling coefficient and critical buckling stress are

$$k_c^Z = \frac{1.277}{2} \left( 1 + \sqrt{1 + 0.0201 * (15)^2} \right) = 2.14$$

$$\sigma_c^Z = k_c^Z \sigma_E = 2.14 * 10.36 = 22.17 \text{ ksi}$$

This elastic critical buckling stress is below the yield strength of aluminum and when compared against the CU-FSM analysis results

$$\sigma_c^Z = 25.8424 \text{ ksi}$$

there is a 14.2% difference. Based upon the variation of the  $R^2$  values, this is a relatively low margin of error between methods.



### (c) Pin-Fixed

The derived equation gives the following critical buckling coefficient and elastic critical buckling stress

$$k_c^Z = \frac{5.42}{2} \left( 1 + \sqrt{1 + .0587 * (15)^2} \right) = 12.92$$

$$\sigma_c^Z = k_c^Z \sigma_E = 12.92 * 10.36 = 133.85 \text{ ksi}$$

where this value is approximately triple the yield stress of aluminum. A CU-FSM analysis yields an elastic critical buckling stress of

$$\sigma_c^Z = 122.1083 \text{ ksi}$$

The elastic critical buckling stress calculated through the derived equation is within 9.62% of the CU-FSM results, indicating a low margin of error.

## 6. CONCLUSION

### 6.1 Summary

Through a series of CU-FSM finite strip analyses, elastic critical buckling stresses of curved aluminum plates over a variety of curvatures are presented. Starting with the concepts covered in LeTran and Davaine's paper concerning curved plate buckling of steel sections, a similar methodology is developed for the determination of an expression for curved plate buckling coefficients and, ultimately, critical buckling stresses. This equation is developed through nonlinear regression analyses employing the *nlinfit* function in MATLAB. The coefficient of determination  $R^2$  is calculated to evaluate the

goodness of fit of the function representing the data points generated through CU-FSM analysis.

The developed equation calculates the critical buckling stress based on the plate buckling coefficient, geometric properties, such as the curvature parameter and width-to-thickness ratio, as well as material properties, including the modulus of elasticity and Poisson's ratio. The equation requires a different parameter for each edge-support condition (pin-pin, pin-fixed, fixed-fixed, fixed-free and pin-free) to increase its applicability.

## 6.2 Conclusions

For aluminum thin plate sections with a defined width, thickness and radius, a simple equation is presented for computing the elastic critical buckling stress resulting from the application of uniform compression over a wide range of edge-support conditions. The critical buckling stress of an element has been determined to be  $\sigma_{cr}^Z = k_c^Z \sigma_E$ , where  $k_c^Z$  can be determined from a simple equation based on edge-support conditions and a curvature parameter  $Z = b^2/Rt$ . Given the width-to-thickness ratio,  $\sigma_E$  can be calculated and used to find the critical buckling stress. These expressions are tested using examples with different geometries, each suggesting reasonable margins of error between the CU-FSM analysis results and the equations generated from the nonlinear regression. This method allows for a single, simple calculation for  $k_c^Z$  instead of running analyses for both curved and flat plate sections to compare ratios. It is

suggested that the next edition of Aluminum Specification consider basing critical buckling stresses on the non-dimensional  $Z$  value to avoid the strict dependency on the  $b/t$  ratio of the section in question.

It is important to note that this study did not consider the effects of initial imperfections and focuses on elastic critical buckling stress, thereby neglecting post-buckling behavior which may be responsible for an increased strength capacity of some sections.

### **6.3 Future Work**

The effects of initial imperfections are not considered in this study and hence, the critical stress procedure presented herein should be considered an upper limit approach with increased similarity between the actual shape and the geometry assumed (Young, 1989). With this in mind, the logical next step to take in this research is to determine the effects of initial imperfections on the strength of the curved sections.

This study only investigates perfect edge-support conditions. The difference between a fixed and a pin support in practice may be difficult to differentiate, and thus partially restrained support conditions should also be considered.

## BIBLIOGRAPHY

Aluminum Association, Specification for Aluminum Structures, Arlington, VA, 2010.

*Extrusion*. (2007, March 7). Retrieved April 20, 2012, from

<http://en.wikipedia.org/wiki/Extrusion>.

Kissell, J.R., and Ferry, R.L., *Aluminum Structures: A guide to their specifications and design*. John Wiley & Sons, Inc., New York, 1995.

Le Tran, Khanh, and Laurence Davaine. "Stability of Curved Panels under Uniform Axial Compression." *Journal of Constructional Steel Research* (2011). Print.

Schafer, B.W., Ádány, S. "Buckling analysis of cold-formed steel members using CUFSM: conventional and constrained finite strip methods." Eighteenth International Specialty Conference on Cold-Formed Steel Structures, Orlando, FL. October 2006.

White, Richard, Peter Gergely, and Robert Sexsmith. *Structural Engineering, Vol. 3, Behavior of Members and Systems*. John Wiley & Sons, Inc., New York, 1974. 87-94. Print.

Young, W.C., *Roark's Formulas for Stress & Strain*. 6<sup>th</sup> ed., McGraw Hill, New York, 1989.

Ziemian, Ronald D. (Ed.). *Guide to Stability Design Criteria for Metal Structures*. 6th ed. Hoboken, NJ: John Wiley & Sons, 2010. Print.

## APPENDIX

### MATLAB Inputs used for Nonlinear Regression

The following command was used for each edge-support condition to calculate the parameter value  $Bhat$  and residuals  $r$  for each case:

$$[Bhat, r] = nlinfit(Z, K_{[boundary\ condition]}, @mdl[boundary\ condition], B0)$$

where  $Z$  is a 20x1 vector of the twenty curvatures investigated,  $K_{[edge-support\ condition]}$  is a 20x1 vector of the twenty corresponding buckling coefficients calculated through CU-FSM at each [edge-support condition]. The input,  $@mdl[edge-support\ condition]$ , calls the function shown below and returns a vector of fitted response values and  $B0$  is an initial guess at the parameter. The MATLAB script below is generalized for the purposes of this example, but [edge-support condition] would be replaced by the label of the edge-support condition case considered.

```
function [y]=mdl[edge-support condition](b,x)
k=4;
y=(k/2*(1+sqrt(1+b*x.^2)));
end
```

In this example,  $y$  is the curved plate buckling coefficient,  $k$  is the plate buckling coefficient,  $b$  is the parameter and  $x$  is the curvature parameter.